

UC Davis

UC Davis Previously Published Works

Title

Structurally related (–)-epicatechin metabolites and gut microbiota derived metabolites exert genomic modifications via VEGF signaling pathways in brain microvascular endothelial cells under lipotoxic conditions: Integrated multi-omic study

Permalink

<https://escholarship.org/uc/item/83m1p0wf>

Authors

Corral-Jara, Karla Fabiola
Nuthikattu, Saivageethi
Rutledge, John
et al.

Publication Date

2022-07-01

DOI

10.1016/j.jprot.2022.104603

Copyright Information

This work is made available under the terms of a Creative Commons Attribution License, available at <https://creativecommons.org/licenses/by/4.0/>

Peer reviewed

Genome Biology

Integrated multi-omic analyses of the genomic modifications by gut microbiome derived metabolites of epicatechin, 5-(4'-Hydroxyphenyl)- γ -valerolactone, in TNF α -stimulated primary human brain microvascular endothelial cells.

--Manuscript Draft--

Manuscript Number:					
Full Title:	Integrated multi-omic analyses of the genomic modifications by gut microbiome derived metabolites of epicatechin, 5-(4'-Hydroxyphenyl)- γ -valerolactone, in TNF α -stimulated primary human brain microvascular endothelial cells.				
Article Type:	Research				
Funding Information:	<table border="1"> <tr> <td>Mars</td> <td>Dr Dragan Milenkovic</td> </tr> <tr> <td>Région Auvergne-Rhône-Alpes (FR)</td> <td>Dr Dragan Milenkovic</td> </tr> </table>	Mars	Dr Dragan Milenkovic	Région Auvergne-Rhône-Alpes (FR)	Dr Dragan Milenkovic
Mars	Dr Dragan Milenkovic				
Région Auvergne-Rhône-Alpes (FR)	Dr Dragan Milenkovic				
Abstract:	<p>Background : The cerebral blood vessels are lined with endothelial and form the blood-brain barrier which dysfunction constitute key event in physiopathology of most neurodegenerative disorders and is also an early event in the aging brain that can contribute to cognitive impairment. Recent studies have suggested that epicatechin can improve various aspects of cognitive functions, lower the risk for developing Alzheimer's disease, decrease the risk of stroke and improve regional cerebral perfusion. However, cellular and molecular mechanisms of epicatechin on brain vascular endothelial cells is still largely unexplored. The objective of this study was to investigate the biological effects of major gut microbiome derived metabolites of epicatechin, 5-(4'-Hydroxyphenyl)-γ-valerolactone-3'-sulfate and 5-(4'-Hydroxyphenyl)-γ-valerolactone-3'-O-glucuronide, in TNF-α-stimulated human brain microvascular endothelial cells at physiology-relevant concentrations and time of exposure by evaluating their multi-omic modification, including expression of protein coding genes, microRNA (miRNA), long non-coding RNAs (lncRNAs) and proteins.</p> <p>Results : Using multi-omics analysis, we observed that gut microbiome derived metabolites are biologically active and can simultaneously modulate expression of protein coding and non-coding (miRNAs and lncRNAs) as well as proteins. Integrative bioinformatic analysis of transcriptome, miRNome, lncRNome and proteome revealed complex network on genomics modifications by acting at different levels of regulation. Metabolites affect cellular pathways such as cell-cell adhesion, cytoskeleton organization, focal adhesion and cell signaling pathways, pathways regulating endothelial permeability and interaction with immune cells.</p> <p>Conclusions : This study demonstrates for the first time complex and multimodal mechanisms of action by which gut microbiome derived epicatechin metabolites can preserve brain vascular endothelial cell integrity, presenting mechanisms of action underlying epicatechin neuroprotective properties.</p>				
Corresponding Author:	Dragan Milenkovic INRA / UC Davis UNITED STATES				
Corresponding Author Secondary Information:					
Corresponding Author's Institution:	INRA / UC Davis				
Corresponding Author's Secondary Institution:					
First Author:	Karla Fabiola Corral Jara				
First Author Secondary Information:					
Order of Authors:	<table border="1"> <tr> <td>Karla Fabiola Corral Jara</td> </tr> <tr> <td>Saivageethi Nuthikattu</td> </tr> <tr> <td>John Rutledge</td> </tr> </table>	Karla Fabiola Corral Jara	Saivageethi Nuthikattu	John Rutledge	
Karla Fabiola Corral Jara					
Saivageethi Nuthikattu					
John Rutledge					

	Amparo Villablanca
	Christine Morand
	Hagen Schroeter
	Dragan Milenkovic
Order of Authors Secondary Information:	
Suggested Reviewers:	<p>Yves Desjardins Professor, University of Laval, Canada Yves.Desjardins@fsaa.ulaval.ca Dr Desjardin is expert in nutrition, health and use of omics</p> <p>David Vauzour senior researcher d.vauzour@uea.ac.uk specialist in molecular nutrition, polyphenols and health</p> <p>Kevin Croft professor kevin.croft@uwa.edu.au Dr Kroft is expert in health effect of polyphenols and mechanism of action</p> <p>Hisanori Kato Organization for Interdisciplinary Research Projects, the University of Tokyo, Tokyo, Japan akatoq@mail.ecc.u-tokyo.ac.jp Dr Kato is specialist in multi-omics analyses related to nutrition research</p>
Additional Information:	
Question	Response
Has this manuscript been submitted to this journal before?	No
<p>Experimental design and statistics</p> <p>Full details of the experimental design and statistical methods used should be given in the Methods section, as detailed in our Minimum Standards Reporting Checklist. Information essential to interpreting the data presented should be made available in the figure legends.</p> <p>Have you included all the information requested in your manuscript?</p>	Yes
<p>Resources</p> <p>A description of all resources used, including antibodies, cell lines, animals and software tools, with enough information to allow them to be uniquely identified, should be included in the Methods section. Authors are strongly</p>	Yes

encouraged to cite [Research Resource Identifiers](#) (RRIDs) for antibodies, model organisms and tools, where possible.

Have you included the information requested as detailed in our [Minimum Standards Reporting Checklist](#) [" target="_blank">Minimum Standards Reporting Checklist?](#)

[Click here to view linked References](#)

1
2
3
4
5
6
7
8
9
10
11
12
13
14
15
16
17
18
19
20
21
22
23
24
25
26
27
28
29
30
31
32
33
34
35
36
37
38
39
40
41
42
43
44
45
46
47
48
49
50
51
52
53
54
55
56
57
58
59
60
61
62
63
64
65

1 **Integrated multi-omic analyses of the genomic modifications by gut microbiome derived**
2 **metabolites of epicatechin, 5-(4'-Hydroxyphenyl)- γ -valerolactone, in TNF α -stimulated**
3 **primary human brain microvascular endothelial cells.**

4
5 Karla Fabiola Corral Jara¹, Saivageethi Nuthikattu², John Rutledge², Amparo Villablanca²,
6 Christine Morand¹, Hagen Schroeter³, Dragan Milenkovic^{2,1,*}

7
8 ¹ Université Clermont Auvergne, INRAE, UNH, F-63000 Clermont-Ferrand, France

9 ² Division of Cardiovascular Medicine, University of California Davis, 95616 Davis, California,
10 USA

11 ³ Mars, Inc., McLean, VA

12
13 * Corresponding author:

14 Dragan Milenkovic, PhD

15 Email: dragan.milenkovic@inrae.fr; dmilenkovic@ucdavis.edu

24

25 **Abstract**

26 **Background:** The cerebral blood vessels are lined with endothelial and form the blood-brain
27 barrier which dysfunction constitute key event in physiopathology of most neurodegenerative
28 disorders and is also an early event in the aging brain that can contribute to cognitive impairment.
29 Recent studies have suggested that epicatechin can improve various aspects of cognitive functions,
30 lower the risk for developing Alzheimer's disease, decrease the risk of stroke and improve regional
31 cerebral perfusion. However, cellular and molecular mechanisms of epicatechin on brain vascular
32 endothelial cells is still largely unexplored. The objective of this study was to investigate the
33 biological effects of major gut microbiome derived metabolites of epicatechin, 5-(4'-
34 Hydroxyphenyl)- γ -valerolactone-3'-sulfate and 5-(4'-Hydroxyphenyl)- γ -valerolactone-3'-O-
35 glucuronide, in TNF- α -stimulated human brain microvascular endothelial cells at physiology-
36 relevant concentrations and time of exposure by evaluating their multi-omic modification,
37 including expression of protein coding genes, microRNA (miRNA), long non-coding RNAs
38 (lncRNAs) and proteins.

39 **Results:** Using multi-omics analysis, we observed that gut microbiome derived metabolites are
40 biologically active and can simultaneously modulate expression of protein coding and non-coding
41 (miRNAs and lncRNAs) as well as proteins. Integrative bioinformatic analysis of transcriptome,
42 miRNome, lncRNome and proteome revealed complex network on genomics modifications by
43 acting at different levels of regulation. Metabolites affect cellular pathways such as cell-cell
44 adhesion, cytoskeleton organization, focal adhesion and cell signaling pathways, pathways
45 regulating endothelial permeability and interaction with immune cells.

1
2
3
4
5
6
7
8
9
10
11
12
13
14
15
16
17
18
19
20
21
22
23
24
25
26
27
28
29
30
31
32
33
34
35
36
37
38
39
40
41
42
43
44
45
46
47
48
49
50
51
52
53
54
55
56
57
58
59
60
61
62
63
64
65

46 Conclusions: This study demonstrates for the first time complex and multimodal mechanisms of
47 action by which gut microbiome derived epicatechin metabolites can preserve brain vascular
48 endothelial cell integrity, presenting mechanisms of action underlying epicatechin neuroprotective
49 properties.

50

1
2
3
4
5
6
7
8
9
10
11
12
13
14
15
16
17
18
19
20
21
22
23
24
25
26
27
28
29
30
31
32
33
34
35
36
37
38
39
40
41
42
43
44
45
46
47
48
49
50
51
52
53
54
55
56
57
58
59
60
61
62
63
64
65

51 **1. Introduction**

52

53 Polyphenols are one of the most abundant phytochemicals found in plant foods. They encompass
54 several families of compounds, with most represented in human diet being phenolic acids and
55 flavonoids [1]. Flavanols are a class of flavonoids found in fruits and exist in a monomeric
56 (catechins and epicatechins), and polymeric (proanthocyanidines) forms. They are commonly
57 found in cocoa, tea and various fruits, such as apple or grape. It has been suggested that they play
58 an important role in the beneficial health effects of fruits, vegetables and derivatives [2].

59 Numerous studies have shown that epicatechin is highly metabolized following its consumption.
60 Epicatechin is absorbed in the small intestine, rapidly conjugated by phase I and phase II
61 detoxification enzymes and appears in the bloodstream from 1 h to 4 h after ingestion with major
62 metabolites such as E3'G, E3'S, 3'ME5S and 3'ME7S [3]. These metabolites are absent from
63 plasma after 6–8 h, at the point when the ingested epicatechin reaches the gastrointestinal (GI)
64 tract and the colon. There, the microbiota induced opening of the C-ring, resulting in the formation
65 of 5-carbon side chain ring fission metabolites that can be further metabolized by the phase II
66 metabolism by enzymes present in the colon and/or the liver resulting in the sulfated and
67 glucuronidated forms of γ -valerolactones that can be detected in plasma. Two major gut
68 metabolites derived catabolites that were identified in plasma are 5-(4'-Hydroxyphenyl)- γ -
69 valerolactone-3'-sulfate and 5-(4'-Hydroxyphenyl)- γ -valerolactone-3'-O-glucuronide, at
70 $272 \pm 56\text{nM}$ and $125 \pm 30\text{nM}$, respectively [3] and can remain in the circulatory system for over
71 12 hours. Very few studies suggested that these γ -valerolactones are bioactive, by exerting anti-
72 inflammatory properties or decreasing blood pressure [4] however such studies remain very scarce.

1
2
3
4
5
6
7
8
9
10
11
12
13
14
15
16
17
18
19
20
21
22
23
24
25
26
27
28
29
30
31
32
33
34
35
36
37
38
39
40
41
42
43
44
45
46
47
48
49
50
51
52
53
54
55
56
57
58
59
60
61
62
63
64
65

73 In the context of health, flavonoids are of particular interest because experimental studies and
74 randomized controlled trials (RCT) have shown that the flavanols exert positive effects on different
75 cardiovascular disease risk factors, including blood pressure, vasodilation or vascular stiffness
76 [5,6]. Hypertension and arterial stiffness are also main risk factors for cerebrovascular injury. The
77 role of cerebrovascular dysfunction in cognitive impairment is increasingly recognized [7]. Its
78 dysfunction can lead to accelerated brain atrophy, reduced cognitive ability, an increased risk of
79 stroke and an increased risk of neurodegenerative diseases, such as Alzheimer's disease (AD), and
80 dementia. Aging impairs the increase in cerebral blood flow triggered by neural activation, known
81 as neurovascular coupling, a complex functional impairment of cerebral microvessels and
82 astrocytes, which likely contribute to neurovascular dysfunction and cognitive decline in aging
83 and in age-related neurodegenerative diseases [8].

84 Several studies suggest that epicatechin can improve various aspects of cognitive function in
85 animals and humans. Flavonoids can preserve cognitive abilities during ageing in rats, lower the
86 risk for developing AD, decrease the risk of stroke in humans, and can exert beneficial effects on
87 cerebral blood flow [9,10]. Protective effects of long-term flavanol consumption on
88 neurocognition and behavior, including age- and disease-related cognitive decline, were shown in
89 animal models of normal aging, dementia, and stroke [11]. A recent systematic review has
90 suggested a positive effect of cocoa polyphenols on memory and executive function [12]. It has
91 also been suggested that consumption of cocoa flavanol may improve regional cerebral perfusion
92 [13] and can also enhance dentate gyrus function and improves cognition in older adults [14].

93 The cerebral blood vessels are lined with endothelial cells (EC) and sealed by tight junctions.
94 Together with astrocytes, pericytes, microglial cells and the basement membrane, they form the
95 blood-brain barrier (BBB) and represent an interactive cellular complex that regulates the entry of

1
2
3
4
5
6
7
8
9
10
11
12
13
14
15
16
17
18
19
20
21
22
23
24
25
26
27
28
29
30
31
32
33
34
35
36
37
38
39
40
41
42
43
44
45
46
47
48
49
50
51
52
53
54
55
56
57
58
59
60
61
62
63
64
65

96 blood products, pathogens and cells into the brain, which is essential for normal neuronal
97 functioning, thus playing an important role in the protection and homeostasis of the brain.
98 Dysfunction of the BBB also plays a key role in most neurodegenerative disorders as BBB
99 dysfunction results in increased permeability of EC, which results in neuro-inflammation that
100 contributes to the neurodegeneration process [15]. BBB degradation is also an early event in the
101 aging human brain that begins in the hippocampus and can contribute to cognitive impairment
102 [16]. It has therefore been suggested that the degradation of BBB is a sensitive and early measure
103 of cognitive dysfunction in Alzheimer's, Parkinson's and even multiple sclerosis [7,17]. We have
104 previously described that epicatechin metabolites can prevent endothelial dysfunction by reducing
105 interactions between monocytes and TNF- α -stimulated vascular EC [18] and also decreasing
106 endothelial permeability [19]. These observations suggest that the observed cognitive and
107 neurological-protective effects of flavanols may be due to their capacity to protect brain-
108 endothelial integrity and BBB permeability.

109 The objective of this study was to investigate the biological effects of major gut microbiome
110 derived metabolites of epicatechin, 5-(4'-Hydroxyphenyl)- γ -valerolactone-3'-sulfate and 5-(4'-
111 Hydroxyphenyl)- γ -valerolactone-3'-O-glucuronide, in TNF- α -stimulated human brain
112 microvascular endothelial cells at physiology-relevant concentrations and time of exposure by
113 evaluating their multi-omic modification, including changes in the expression of protein coding
114 genes, non-coding microRNA (miRNA) and long non-coding RNAs (lncRNAs) genes together
115 with proteomics modifications.

116
117 **2. Materials and methods**
118

1
2
3
4 **119 2.1 Compounds**

5
6 **120** Epicatechin gut microbiota metabolites: 5-(4'-Hydroxyphenyl)- γ -valerolactone-3'-sulfate
7
8
9 **121** (γ VL3'G) and 5-(4'-Hydroxyphenyl)- γ -valerolactone-3'-O-glucuronide (γ VL3'S) were gifted by
10
11 **122** Mars, Inc. Chemical structures are presented in the Supplemental Figure 1. Stock solutions of γ -
12
13
14 **123** valerolactones were prepared by dissolving them in 50% ethanol at 2mM and stored at -80°C until
15
16 **124** assayed. For the cell treatments, a mixture of compounds was used in proportion of 0.65/0.35 for
17
18
19 **125** γ VL3'S and γ VL3'G, respectively. Once dissolved in the culture medium, the final concentration
20
21 **126** for γ VL3'S was 650nM and γ VL3'G was 350nM, with total final concentration of 1 μ M.
22

23
24 **127**
25
26 **128 2.2 Cell culture**

27
28 **129** Human brain microvascular endothelial cells (HBMEC) were obtained from Angio-Proteomie
29
30
31 **130** (Boston, MA, USA). Cells were cultured in the EBM-2 Endothelial Cell Growth Basal Medium
32
33 **131** supplemented with 2% fetal bovine serum, 0.4 % human fibroblast growth factor, 0.1% human
34
35
36 **132** epidermal growth factor, 0.1% insulin-like growth factor, 0.1% vascular endothelial growth factor,
37
38 **133** 0.1% heparin, 0.1% ascorbic acid, 0.1% gentamicin/amphotericin-B and 0.04% hydrocortisone,
39
40
41 **134** all from Lonza (Walkersville, MD, USA). Cell cultures were maintained at 37°C and 5% CO₂.
42
43 **135** HBMECs were used at the passage 4. The cells, 50000 cells/well, were seeded on 24-well plates
44
45
46 **136** (Becton Dickinson, USA) that were coated with collagen (Cell Applications, San Diego, CA,
47
48 **137** USA). At 80% of confluence, cells were exposed to the mixture of gut metabolites for 20h. Cells
49
50 **138** treated with medium containing 0.01% ethanol final concentration was used as controls. After the
51
52
53 **139** incubation, the medium was discarded, and inflammatory stress was induced by 4h-incubation
54
55 **140** with 1ng/ml of TNF- α (VALs group) (R&D Systems, MN, USA). Cells treated with medium only
56
57
58
59
60
61
62
63
64
65

1
2
3
4
5
6
7
8
9
10
11
12
13
14
15
16
17
18
19
20
21
22
23
24
25
26
27
28
29
30
31
32
33
34
35
36
37
38
39
40
41
42
43
44
45
46
47
48
49
50
51
52
53
54
55
56
57
58
59
60
61
62
63
64
65

141 and incubated with TNF- α were used as control (TNF- α group). Negative control cells (control
142 group) were treated with medium and no TNF- α incubation.

143
2.3 RNA extraction
144
145 Total RNA, including short RNAs as miRNAs, were extracted using Monarch® Total RNA
146 Miniprep Kit (New England BioLabs, USA) following manufacture's instruction. Briefly, cells
147 were lysed using a lysis buffer and genomic DNA was removed by centrifugation in gDNA
148 removal columns. RNA was then fixed to the RNA purification column, a step that was followed
149 by successive steps of washing and centrifugations. At the end, total RNA was eluted using
150 nuclease free water. RNA quality and quantity were checked by agarose gel electrophoresis and
151 determination of the absorbance ratio at 260/280 nm using NanoDrop ND-1000 spectrophotometer
152 (Thermo Scientific, Wilmington, DE, USA). The total RNA samples were stored at -80°C until
153 used.

2.4 Microarray analysis of mRNA, miRNA, snoRNA and lncRNA expression
155
156 For transcriptomics analysis, we used Affymetrix Clariom D array for human, containing over 6
157 million probes for protein coding genes but also protein non-coding genes such as miRNAs,
158 lncRNAs and small nucleolar RNAs (snoRNAs) (Thermo Fisher Scientific, Santa Clara, CA).
159 RNA (100 ng) was used to prepare cRNA and sscDNA using Thermo Fisher Scientific GeneChip®
160 WT PLUS reagent Kit. SscDNA (5.5 ug) was fragmented by uracil-DNA glycosylase (UDG) and
161 apurinic/apyrimidinic endonuclease 1 (APE 1) and labeled by terminal deoxynucleotidyl
162 transferase (TdT) using the DNA Labeling Reagent that is covalently linked to biotin. Fragmented
163 and labelled ssCDNA samples in triplicate were then submitted to the UC Davis Genome Center

1
2
3
4
5
6
7
8
9
10
11
12
13
14
15
16
17
18
19
20
21
22
23
24
25
26
27
28
29
30
31
32
33
34
35
36
37
38
39
40
41
42
43
44
45
46
47
48
49
50
51
52
53
54
55
56
57
58
59
60
61
62
63
64
65

164 shared resource core for hybridization, staining, and scanning using Thermo Fisher Scientific WT
165 array hybridization protocol following the manufacturer's protocol. Hybridization of fragmented
166 and labelled ssCDNA samples was done using GeneChip™Hybridization Oven and samples were
167 then washed and stained using GeneChip™ Fluidics Station. The arrays were scanned using
168 GeneChip™ Scanner 3000 7G (Thermo Fisher Scientific, Santa Clara, CA). Quality control of the
169 microarrays and data analysis were performed using Thermo Fisher Scientific Transcriptome
170 Analysis Console software version 4.0.2. Pair-wise comparisons between biological conditions
171 were applied using specific contrasts. A correction for multiple testing was applied using
172 Benjamini-Hochberg procedure (BH, Benjamini et al. 1995, pubmed ID 24913697) to control the
173 False Discovery Rate (FDR). Probes with FDR-adjusted $P < 0.05$ were considered to be
174 differentially expressed between conditions. All raw and normalized data are available in GEO
175 database under accession series number: GSE156116.

2.5 Proteomics analysis

178 The global proteomics analysis was performed as previously described [20]. Briefly, to prepare
179 the samples, 4 per group, cells were homogenized in lysis buffer and the protein concentration of
180 the supernatant was measured using Bicinchoninic Acid (BCA) protein assay. One hundred µg of
181 protein sample was denatured, precipitated and the supernatant was discarded, and pellet was air
182 dried. The proteins were then digested and concentrated and labelled using TMT 10-plex peptide
183 labeling (Thermo Scientific, Canoga Park, CA, US). All TMT labeled samples were combined in
184 equal amounts. LC separation was done on a Dionex Nano Ultimate 3000 (Thermo Scientific) with
185 a Thermo Easy-Spray source. Mass spectra were collected on a Fusion Lumos mass spectrometer
186 (Thermo Fisher Scientific) in a data-dependent MS3 synchronous precursor selection (SPS)

1
2
3
4
5
6
7
8
9
10
11
12
13
14
15
16
17
18
19
20
21
22
23
24
25
26
27
28
29
30
31
32
33
34
35
36
37
38
39
40
41
42
43
44
45
46
47
48
49
50
51
52
53
54
55
56
57
58
59
60
61
62
63
64
65

187 method. MS1 spectra were acquired in the Orbitrap, 120 K resolution, 50 ms max inject time, 5
188 $\times 10^5$ max inject time. MS2 spectra were acquired in the linear ion trap with a 0.7 Da isolation
189 window, CID fragmentation energy of 35%, turbo scan speed, 50 ms max inject time, 1×10^4
190 automatic gain control (AGC) and maximum parallelizable time turned on¹⁷. MS2 ions were
191 isolated in the ion trap and fragmented with a HCD energy of 65%. MS3 spectra were acquired in
192 the orbitrap with a resolution of 50K and a scan range of 100–500 Da, 105 ms max inject time and
193 1×10^5 AGC.

194 *Quantitative data analysis:* The 4 samples of cells treated with metabolites and 4 vehicle treated
195 samples were used for isobaric-labeled LC-MS/MS quantitative measurements. These factors
196 include ratio compression and can cause an underestimation of changes in relative abundance of
197 proteins across samples. Raw files were processed with Proteome Discoverer 2.2 (Thermo
198 Scientific) using the default MS3 SPS method with the following modifications for importation
199 into Scaffold Q+. Target Decoy PSM validator was used instead of Percolator and Maximum Delta
200 Cn was set to 1. All MS/MS samples were analyzed using Sequest HT to search all mouse
201 sequences from Uniprot (<https://www.uniprot.org/proteomes/UP000000589>) and 110 common
202 laboratory contaminants (<http://thegpm.org.crap>) plus an equal number of reverse decoy sequences
203 assuming the digestion enzyme trypsin. Sequest-HT was searched with a fragment ion mass
204 tolerance of 0.20 Da and a parent ion tolerance of 10.0 PPM. Carbamidomethyl of cysteine and
205 TMT10 plex of lysine were specified in Sequest-HT as fixed modifications. Oxidation of
206 methionine and acetyl of the n-terminus were specified in Sequest-HT as variable modifications.
207 Scaffold Q+ (version Scaffold_4.9.0, Proteome Software Inc., Portland, OR) was used to
208 quantitate Label Based Quantitation (iTRAQ, TMT, SILAC, etc.) peptide and protein
209 identifications. Peptide identifications were accepted with a decoy false FDR cutoff of less than

1
2
3
4
5
6
7
8
9
10
11
12
13
14
15
16
17
18
19
20
21
22
23
24
25
26
27
28
29
30
31
32
33
34
35
36
37
38
39
40
41
42
43
44
45
46
47
48
49
50
51
52
53
54
55
56
57
58
59
60
61
62
63
64
65

210 0.2%. Protein identifications were accepted if they could be established with at least 2 unique
211 identified peptides. Proteins that contained similar peptides and could not be differentiated based
212 on MS/MS analysis alone were grouped to satisfy the principles of parsimony. Normalization was
213 performed iteratively (across samples and spectra) on intensities, as described in Statistical
214 Analysis of Relative Labeled Mass Spectrometry Data from Complex Samples using ANOVA.
215 Medians were used for averaging and spectra data were log-transformed and weighted by an
216 adaptive intensity weighting algorithm.

218 **2.6 Bioinformatic analysis and multi-omics integration**

219 **2.6.1. Genes, targets and proteins distribution plots**

220 Data visualization was performed in Manhattan plots to show chromosomal localizations of
221 differentially expressed transcripts and Venn Diagrams to show all possible logical relations
222 between multiple omic sets. Venn diagrams were used to visualize the relationships between
223 differentially expressed (DE) protein-coding genes (mRNAs), miRNA targets, lncRNA targets and
224 DE proteins observed in TNF- α vs control and VALs vs TNF- α group comparisons. Both plots,
225 Manhattan and Venn diagram, were built using R software packages, the Sushi package (Phanstiel,
226 2019, 24903420) and the VennDiagram package (Chen and Boutros, 2011, 21269502),
227 respectively. Conversely, associations between genes and groups were searched using
228 unsupervised hierarchical clustering of the samples and the differentially expressed probes using
229 the Pearson correlation as distance metric and Ward' s method for agglomeration of clusters. The
230 clustering results were illustrated as a heatmap of expression signals. We used the software Permut
231 Matrix to construct the heatmaps (<http://www.atgc-montpellier.fr/permutmatrix/>, Caraux and
232 Pinloche, 2005).

1
2
3
4
5
6
7
8
9
10
11
12
13
14
15
16
17
18
19
20
21
22
23
24
25
26
27
28
29
30
31
32
33
34
35
36
37
38
39
40
41
42
43
44
45
46
47
48
49
50
51
52
53
54
55
56
57
58
59
60
61
62
63
64
65

233

2.6.2. Databases-predicted miRNA targets

For each miRNA identified as differentially expressed in TNF- α vs control and VALs vs TNF- α group comparisons, we performed a target analysis. miRNA targets were predicted using three prediction databases miRTarBase [21], mirRDB [22], and TargetScan [23], and only targets identified in at least two of the databases were considered as putative targets for our analysis. For each database we always chose the most stringent option among those proposed by the database.

240

2.6.3. Databases-predicted lncRNA targets

For each lncRNA identified as differentially expressed in TNF- α vs control and VALs vs TNF- α group comparisons, we also performed a target analysis. lncRNA target transcripts were predicted by combining the results of two prediction databases from Rtools web server: lncRRISearch (<http://rtools.cbrc.jp/LncRRISearch>) [24] and RNARNA (<http://rtools.cbrc.jp/cgi-bin/RNARNA/index.pl>). Targets identified in these two databases were considered as putative targets and used in our analysis. For each database we always chose the most stringent option among those proposed by the database.

249

2.6.4. Protein-protein interactions

In order to perform Protein-Protein Interaction Networks Functional Enrichment Analysis we used STRING database [25] (<https://string-db.org/>).

253

2.6.5. Transcription factors analysis

1
2
3
4
5
6
7
8
9
10
11
12
13
14
15
16
17
18
19
20
21
22
23
24
25
26
27
28
29
30
31
32
33
34
35
36
37
38
39
40
41
42
43
44
45
46
47
48
49
50
51
52
53
54
55
56
57
58
59
60
61
62
63
64
65

255 Transcription factors (TFs) potentially involved in the regulation of the expression of identified
256 mRNAs and which activity can be affected by epicatechin metabolites were searched using
257 enrichR online tool (<https://amp.pharm.mssm.edu/Enrichr/>) [26]. The TFs were also searched
258 within TRRUST (transcriptional regulatory relationships unravelled by sentence-based text-
259 mining) database, a manually curated database of human and mouse transcriptional regulatory
260 networks that contains 8,444 and 6,552 TF-target regulatory relationships of 800 human TFs and
261 828 mouse TFs, respectively that have been derived from 11,237 pubmed articles.

2.6.6. Docking analysis

264 Molecular docking analysis was employed to explore the potential interaction/binding between
265 identified transcription factors and cell signaling proteins regulating the activity of the
266 transcription factors identified and the 2 metabolites, 5-(4'-Hydroxyphenyl)- γ -valerolactone-3'-
267 sulfate (γ VL3'G) and 5-(4'-Hydroxyphenyl)- γ -valerolactone-3'-O-glucuronide (γ VL3'S). The 3D
268 structures of metabolites were obtained from PubChem database
269 (<https://pubchem.ncbi.nlm.nih.gov>) and the three-dimensional structure of the proteins was
270 obtained from the Protein Data Bank (PDB) database. Docking calculations were carried out using
271 Blind Docking server (<https://bio-hpc.ucam.edu/achilles>) [27].

2.6.7. Pathway analysis

274 *Pathway enrichment analysis.* Cellular pathways from TNF- α vs control and VALs vs TNF- α
275 group comparisons were explored using GeneTrail2 (<https://genetrail2.bioinf.uni-sb.de/>) [28]. The
276 lists of significantly regulated mRNAs, miRNA targets, lncRNA targets and significantly regulated
277 proteins, separately or together, were used to identify enrichment of biological categories using an

1
2
3
4 278 over-representation analysis or gene set enrichment analysis (GSEA) with threshold fixed at $P <$
5
6
7 279 0.05 using the Benjamini-Yekutieli correction (as recommended by GeneTrail2). KEGG, Biocarta
8
9 280 and Wiki pathways were evaluated in the analysis.
10
11 281 *Pathways network.* The enriched pathways obtained in our previous step were used to build a
12
13
14 282 network of pathways; two pathways were considered interconnected if at least one of the genes or
15
16 283 hits involved in them were common to both. Networks were constructed and visualized using
17
18
19 284 Cytoscape software (version 3.7.1; <http://www.cytoscape.org/>) [29]. Data preparation was
20
21 285 performed with the use of several R packages included splitstackshape
22
23 286 (<https://github.com/mrdwab/splitstackshape>), data.table (<https://github.com/Rdatatable>
24
25
26 287 /data.table), dplyr (<http://dplyr.tidyverse.org>,<https://github.com/tidyverse/dplyr>) and string
27
28
29 288 (<http://stringr.tidyverse.org>, <https://github.com/tidyverse/stringr>). Pathway networks were built
30
31 289 separately for pathways enriched in each omic layer and pathways obtained from a global pathway
32
33 290 enrichment analysis, considering all omic layers components together. To obtain the 6 pathways
34
35
36 291 with the highest degree (number of connections of one node to other nodes), the Cytoscape
37
38 292 Network Analyzer application was used (<http://apps.cytoscape.org/apps/networkanalyzer>).
39
40
41 293 *Networks of pathways related with endothelial function.* Endothelial function pathways-related
42
43 294 were selected to construct a network. Endothelial function pathway-specific network was
44
45
46 295 performed in Cytoscape software. As a first step we obtained a list of genes involved in selected
47
48 296 pathways from Kyoto Encyclopedia of Genes and Genomes (KEGG) database [30]. Subsequently,
49
50
51 297 through a series of intersections and non-intersections functions in R, we obtained the mRNAs and
52
53 298 proteins involved in the endothelial function pathways, which were also identified to be
54
55 299 differentially expressed in our study. Finally, we identified endothelial function pathway
56
57
58 300 components that were targets of miRNAs or lncRNAs.
59
60
61
62
63
64
65

1
2
3
4
5
6
7
8
9
10
11
12
13
14
15
16
17
18
19
20
21
22
23
24
25
26
27
28
29
30
31
32
33
34
35
36
37
38
39
40
41
42
43
44
45
46
47
48
49
50
51
52
53
54
55
56
57
58
59
60
61
62
63
64
65

301

302 **2.6.8. Multilayer integration and representation**

303 *mRNA, miRNA, lncRNA, proteins and targets interaction networks.* Visualization of the
304 interactions between mRNA-TFs, miRNAs-targets, lncRNA-targets and protein-protein were
305 performed in Cytoscape software. Separate networks for each omic layer and a global network
306 with all integrated interactions were made. Smaller networks were constructed to represent the
307 miRNA targets, lncRNA targets and DE proteins intersected with mRNAs DE in our study.

308 *mRNA, miRNA, lncRNA, proteins and targets interaction networks of focal adhesion pathway.* We
309 identified quantitatively changed mRNAs, miRNAs and their targets, lncRNAs and their targets,
310 together with proteins DE in our study and mapped them to the global map provided in KEGG
311 pathway database, to include a comprehensive pathway topology.

312

313

1
2
3
4
5
6
7
8
9
10
11
12
13
14
15
16
17
18
19
20
21
22
23
24
25
26
27
28
29
30
31
32
33
34
35
36
37
38
39
40
41
42
43
44
45
46
47
48
49
50
51
52
53
54
55
56
57
58
59
60
61
62
63
64
65

314 **3. Results**

315 **3.1 TNF- α modulates expression of protein coding and non-coding genes and proteins in** 316 **HBMEC cells**

317 Firstly, we aimed to assess the effect of TNF- α , in comparison to control group without TNF- α ,
318 on the expression of genes, both protein-coding and non-coding transcripts, using transcriptomics
319 microarray, as well as the effect on protein expression using shotgun proteomics. Regarding the
320 effect on gene expression, from 135,751 total probes, 751 were identified as differentially
321 expressed, at least 0.55%, since some probes were discarded during data cleaning treatment.
322 Manhattan plot showed a uniform distribution of the transcripts on the chromosomes (Figure 1A).
323 We found that of the total differentially expressed transcripts, 85.5% correspond to protein-coding
324 genes (642 mRNAs), 1.89% to miRNAs (23 miRNAs) and 7.07% to lncRNAs (86 lncRNAs)
325 (Figure 1B). Regarding proteomic data, we observed an 8.3% differentiation rate, that is, 464
326 significantly differentially expressed proteins out of a total of 5565 (Figure 1B).

327 Subsequently, miRNAs and lncRNAs target gene predictions from the database analysis identified
328 4125 miRNA targets and 239 lncRNA targets. Thirty-one of these targets were shared between
329 both omic layers (miRNA and lncRNA targets), of which 3 corresponded to mRNA and 1 to
330 protein category. The number of component intersections between all omic layers is shown in
331 Figure 1C. For instance, 175 miRNAs targets belong to mRNAs category, 3 of them are shared by
332 lncRNA targets and 6 by proteins, 6 total lncRNA targets belong to mRNA category, and 24 total
333 proteins belong to the category of mRNAs.

334 We extrapolated the nutrigenomic modification data to build a network of interactions, that is
335 considering DE mRNAs, DE miRNA and their targets, DE lncRNA and their targets, and DE
336 proteins. The global network with all the interactions is shown in Figure 1D. The simplified version

1
2
3
4
5
6
7
8
9
10
11
12
13
14
15
16
17
18
19
20
21
22
23
24
25
26
27
28
29
30
31
32
33
34
35
36
37
38
39
40
41
42
43
44
45
46
47
48
49
50
51
52
53
54
55
56
57
58
59
60
61
62
63
64
65

337 of global network is shown in Figure 1E, miRNA targets, lncRNA targets and proteins and that
338 belong to DE mRNAs omic layer were considered (at least 196 components as shown in Figure
339 1C).The components of each category with the highest degree of connections are: (i) miRNAs:
340 hsa-miR-146-3p, hsa-miR-214-3p, hsa-miR-7844-5p, hsa-miR-6732-3p and hsa-miR-155-5p, (ii)
341 lncRNAs: RP11-274H2.3, RP11-258C19.7, AC098617.1, RP11-373D23.3, RP11-661013.1, (iii)
342 mRNAs: ATP6V1C1, QKI, ANTXR2, TRAF3, TNPO1.

343 For functionality analysis, each omic layer's components were used to perform an enrichment
344 analysis and obtain pathways related to mRNAs, miRNA targets, lncRNA targets and proteins
345 differentially expressed in our study, as presented in the multicolored histogram in Figure 2A. This
346 analysis shows that differentially expressed genes and proteins can impact the cellular functions
347 regulating cell signaling (Toll like receptor signaling pathways, Ras signaling pathway, NF-
348 kappaB (NF-κB) signaling pathway or PI3K-Akt signaling pathway), cell-cell adhesions (cell
349 adhesion molecules pathway or adherent junctions), chemotaxis (chemokine signaling pathway,
350 cytokine-cytokine receptor interaction) or cellular metabolism (citrate cycle, amino acid
351 metabolism or sucrose metabolism). Certain pathways were enriched with miRNA targets such as
352 Notch signaling pathways, RNA transport, spliceosome; or from lncRNA targets such as purine
353 metabolism and tight junction. Some pathways such as TNF-α and NF-κB signaling were enriched
354 by components of mRNAs and proteins categories; 2-Oxocarboxylic acid metabolism by miRNA
355 and lncRNA targets; and regulation of autophagy by mRNA and miRNA components.

356 Thenceforward, we constructed a network of interactions between mRNAs, miRNA-targets,
357 lncRNA-targets, and proteins mapped to genes of pathways of endothelial related functions, such
358 as focal adhesion, tight/adherent junctions, or actin cytoskeleton organization (Figure 2B). From
359 1,392 genes totally involved in endothelial functional pathways, 113 mRNAs and 24 proteins were

1
2
3
4
5
6
7
8
9
10
11
12
13
14
15
16
17
18
19
20
21
22
23
24
25
26
27
28
29
30
31
32
33
34
35
36
37
38
39
40
41
42
43
44
45
46
47
48
49
50
51
52
53
54
55
56
57
58
59
60
61
62
63
64
65

360 differentially expressed in our study. Next, endothelial-related genes were used to search for their
361 regulation by miRNAs or lncRNAs, and 402 miRNA regulations and 15 lncRNA regulations were
362 found. Some of these interactions that may be related to endothelial functions were hsa-miR-7844-
363 5p-TRAF3, REL-VCAM1, VCAM1-ICAM1, for instance. These data suggest that TNF- α can
364 affect EC functions, such as cell adhesion, junctions or cell signaling, through multi-level mode of
365 genomic regulations, simultaneously affecting mRNA, miRNA, lncRNAs and proteins.

367 **3.2 γ -valerolactones can modulate expression of genes and proteins in HBMEC**

368 In order to evaluate the effect of γ -valerolactones (VALs) on the transcriptomic and proteomic
369 expression in brain microvascular endothelial cells, a microarray and shotgun analysis were also
370 performed. We compared the global gene expression profiles of the 3 study groups (Figure 3A)
371 using PLSDA analysis and observed that the VALs groups had different expression profiles from
372 the TNF- α and control groups. This observation suggests changes in expression profile in HBMEC
373 following exposure to the VALs.

374 Statistical analysis was then performed to identify differentially expressed transcripts. The
375 percentage of transcripts DE in cells treated with TNF- α + VALs (VALs group) vs TNF- α alone
376 (TNF- α group) was 0.15%, that is 211 transcripts. Integrally, 19.67% of these modifications
377 correspond to protein-coding genes (61 mRNAs), 1.93% to miRNAs (6 miRNAs), 25.48% to
378 lncRNAs (79 lncRNAs) (Figure 3B). On the other hand, proteomics analysis indicates 2.94% of
379 differentiated proteins, corresponding to 52.90% (164 proteins) of total transcripts and proteins
380 DE (Figure 3B). A Manhattan plot of transcripts shows that differentially expressed genes are
381 localized throughout the genomes (Figure 3C). The expression profile of genes identified in VALs
382 group was compared with expression profile of genes identified as differentially expressed by

1
2
3
4
5
6
7
8
9
10
11
12
13
14
15
16
17
18
19
20
21
22
23
24
25
26
27
28
29
30
31
32
33
34
35
36
37
38
39
40
41
42
43
44
45
46
47
48
49
50
51
52
53
54
55
56
57
58
59
60
61
62
63
64
65

383 TNF- α group and presented by a heat map, Figure 3D. This analysis revealed that over half of
384 VALs genes present opposite expression profile when compared to TNF- α group, that is genes
385 identified as up-regulated by exposure of cells to TNF- α were identified as down-regulated by
386 VALs and inversely, genes identified as down-regulated by TNF- α were identified as up-regulated
387 by VALs. This observation suggests that exposure of HBMEC to VALs can, at least partially,
388 counteract the inflammatory stress induced by TNF- α .
389 Furthermore, these data suggest for the first time that epicatechin gut microbiota metabolites have
390 capacity to exert complex genomic modification. These effects however seem to be of lesser
391 impact on genomic and proteomics modifications than of TNF- α effect.

392

3.2.1. γ -valerolactones modulate expression of protein-coding genes in HBMEC

394 In order to seek the functional pathways that could be modulated by DE protein-coding genes
395 (Supplemental Table 1) in our VALs study group vs TNF- α group, we performed an enrichment
396 analysis in GeneTrail. This analysis showed that mRNAs are involved in different processes
397 regulating cell adhesion and permeability (Gap junction, Tight junction, Focal adhesion, Adherens
398 junction, Leukocyte transendothelial migration pathways), cell signaling (Rap1 signaling, Thyroid
399 hormone signaling, Wnt signaling, PI3K-Akt signaling), cell metabolism (Glycosphingolipid
400 biosynthesis, TCA cycle, Amino sugar and nucleotide sugar) and other pathways, as shown in
401 Figure 4A. Subsequently, we constructed a network in order to integrate and show connections
402 between the pathways resulting from our previous analysis (Figure 4B). Three clusters were
403 observed, the largest including Rap1, Wnt, and PI3K-Akt signaling pathways strongly connected
404 with leukocyte transendothelial migration, adherent junction, tight junction and gap junction. The
405 two smallest consist of a cluster that involves glycosphingolipid biosynthesis, amino sugar and

1
2
3
4
5
6
7
8
9
10
11
12
13
14
15
16
17
18
19
20
21
22
23
24
25
26
27
28
29
30
31
32
33
34
35
36
37
38
39
40
41
42
43
44
45
46
47
48
49
50
51
52
53
54
55
56
57
58
59
60
61
62
63
64
65

406 nucleotide sugar metabolism and glycosaminoglycan degradation. We can clearly observe a
407 separation of the processes related to cellular metabolism and those of cell-cell contact regulation.
408 The pathways with the highest degree of interaction with other pathways are Wnt signaling, Rap1
409 signaling, tight junction and hippo signaling pathway. Consequently, this observation suggests that
410 γ -valerolactones exposure could modulate endothelial cells function, that is adhesion with immune
411 cells but also endothelial cell permeability, by regulating of mRNAs, miRNAs, lncRNAs and
412 proteins involved in these processes.

3.2.2. γ -valerolactones modulate the expression of miRNA in HBMEC

415 MiRNA expression was also identified as modulated following exposure of HBMEC to γ -
416 valerolactones, suggesting the capacity of these metabolites at physiologically-relevant
417 concentrations to modulate the expression of small non-coding RNAs (Supplemental Table 2).
418 Search for their putative targets from the databases for 6 differentially expressed miRNAs, hsa-
419 miR-6730-3p, hsa-miR-6730-5p, hsa-miR-3661-3p, hsa-miR-3661-5p, hsa-miR-6746-3p, hsa -
420 miR-6746-5p, allowed us to identify 1360 target genes, including ARSB, CXADR, FREM1 or
421 HAP1. Among them, 5 targets are in common with differential expression mRNA (Supplemental
422 Figure 3A). Figure 5A shows network topology of miRNA-target interactions which revealed at
423 least four miRNA hubs for the hsa-miR-6730-5p, hsa-miR-6730-3p, hsa-miR-6746-5p and has-
424 miR-6746-3p.

425 Likewise, miRNA targets functionality analysis was performed by placing these genes into cellular
426 pathways. MiRNAs targets have been found to play a role in pathways such as those regulating
427 EC functions (adherent junction, gap junction, focal adhesion), cell signaling (PI3K-Akt, Wnt,
428 Foxo, MAPK, PPAR signaling) or cell metabolism (pyrimidine, purine and protein digestion

1
2
3
4
5
6
7
8
9
10
11
12
13
14
15
16
17
18
19
20
21
22
23
24
25
26
27
28
29
30
31
32
33
34
35
36
37
38
39
40
41
42
43
44
45
46
47
48
49
50
51
52
53
54
55
56
57
58
59
60
61
62
63
64
65

429 metabolism) (Figure 5B). Thirty-six resulting pathways were found in turn in mRNAs enrichment
430 analysis (Supplemental Figure 3B), this suggests that although only few targets are shared in both
431 omic layers (mRNA and miRNA targets), their functionality is similar. In Supplemental Figure 2,
432 the connections between miRNA targets-related pathways are shown, where centrality is one of
433 its characteristics. We observed that the pathways with the highest degree of interaction with others
434 are pathways in Ras signaling pathway, PI3K-Akt signaling, FOXO signaling, viral carcinogenesis
435 and MAPK signaling pathway.

3.2.3. lncRNA expression modulation by γ -valerolactones

438 Microarray analysis have also shown for the first time that exposure of HBMEC to γ -
439 valerolactones can also modulate expression of another group of protein non-coding RNA, which
440 are long-non-coding RNAs. We observed change in expression of 79 lncRNAs (Supplemental
441 Table 3). Search of databases for their targets allowed us to identify 364 lncRNA-targets. Among
442 these 364 targets, 4 (UBC, C11orf95, PLCB1, BHLHE40) are in common with protein coding
443 genes and 14 (IL6ST, ABHD12, HIPK2, PLEKHG2, PSD4, ZNF37A, AMOT, POU4F1, UBC,
444 CELF3, AGO1, EFNA3, BCL7A, PRDM2) with miRNAs targets (Supplemental Figure 3A). In
445 Figure 6A lncRNA-targets interactions topology is shown which identified several clusters of
446 genes, such as for lncRNA RP11-386G11.10, RP11-192H23.7, AC012668.2, FTX, AC005562.1
447 or lncRNAs hubs.

448 In lncRNAs targets functionality analysis, we observed an enrichment of pathways involved in the
449 regulation of EC (gap junction, focal adhesion, ECM-receptor interaction, regulation of actin
450 cytoskeleton, Rap1 signaling pathways), cellular metabolism (PI3K-AKT, calcium, PPAR, NF-
451 κ B, JAK-STAT, mTOR signaling pathways) or cell signaling (carbon, purine, pentose phosphate,

1
2
3
4
5
6
7
8
9
10
11
12
13
14
15
16
17
18
19
20
21
22
23
24
25
26
27
28
29
30
31
32
33
34
35
36
37
38
39
40
41
42
43
44
45
46
47
48
49
50
51
52
53
54
55
56
57
58
59
60
61
62
63
64
65

glycolysis, gluconeogenesis metabolism) (Figure 6B). We can corroborate that most of the pathways described are themselves the result of mRNA and miRNA targets pathway analysis. Sixteen pathways were shared with protein-coding genes enrichment analysis, while 37 are shared with miRNAs pathways analysis (Supplementary Figure 3B).

In order to analyze the connections between these pathways, we built a network of interactions presented in Figure 6C. We observed a strong relationship between intracellular signaling pathways, PPAR, NF- κ B, PI3K-Akt, Rap1 signaling, with focal adhesion and gap junction. These pathways were grouped in a large cluster, connected with a smaller cluster in which inflammatory and cytokine pathways were involved. Metabolic processes were grouped in a separate cluster. The pathways with the highest degree of connections with other pathways are Rap1 signaling, Focal adhesion, long term potentiation, microRNAs in cancer, phagosome and gap junction. Taken together, this study shows for the first time the capacity of γ -valerolactones to modulate the expression of miRNAs and lncRNAs, particularly those involved in the regulation of endothelial cell function and permeability.

466

3.2.4. Proteomics modulation by γ -valerolactones

Use of proteomic untargeted shotgun approach allowed us to demonstrate that exposure of HBMEC to γ -valerolactones can also affect the expression of proteins (Supplemental Table 4). We observed that γ -valerolactone metabolites modulated the expression of 164 different proteins. Functional analyses revealed that these proteins play a role in pathways related to cell metabolic pathways, cell signaling pathways and others, as shown in Figure 7A. In metabolic processes we observed that valine, leucine and isoleucine biosynthesis, 2-oxocarboxylic acid, biosynthesis of unsaturated fatty acids, glycosaminoglycan degradation were part of this category. The interactions

1
2
3
4
5
6
7
8
9
10
11
12
13
14
15
16
17
18
19
20
21
22
23
24
25
26
27
28
29
30
31
32
33
34
35
36
37
38
39
40
41
42
43
44
45
46
47
48
49
50
51
52
53
54
55
56
57
58
59
60
61
62
63
64
65

475 between pathways is shown in Figure 7B. The pathways with the highest degree of connections
476 with other pathways are renal cell carcinoma, prostate cancer, or natural killer cell mediated
477 cytotoxicity.

478 **3.2.5. Transcription factor and interactome analysis using 3D in-silico modeling for γ - 479 valerolactones**

480 Using gene expression analysis data, Ttrust database was searched using EnrichR tool to identify
481 potential TFs whose activity could be affected by γ -valerolactones and involved in the observed
482 changes in the expression of genes. Among the most significant TFs identified were NF- κ B1,
483 cJUN, STAT2, IRF1, or FOXO4 (Figure 8A). Following this analysis, we aimed to identify if γ -
484 valerolactones could have binding affinity with these TFs, binding that may affect their activity
485 and consequently result in changes in expression of genes as we observed. Using this approach,
486 we observed that γ -valerolactones have potential to bind to transcription factor, interaction that
487 could affect their activity and induce changes in expression of genes, as observed using our
488 microarray analysis. The analysis suggests that glucuronidated form of γ -valerolactone has slightly
489 higher potential to bind to protein tested than sulfated metabolite. The highest binding was
490 observed between γ VL3'G and RelA protein, with binding free energy identified being -7kcal/mol
491 (Figure 8B), followed by its binding to NF- κ B (-6.9kcal/mol). γ VL3'S showed highest binding
492 capacity with RelA (binding energy of -6.6kcal/mol) (Figure 8C).

493 **3.3. Integration of multi-omics data of γ -valerolactones treatment in HBMEC cells**

494 As a first step towards data integration, we grouped mRNA, miRNA targets, lncRNA targets, and
495 protein interactions from their individual analyses into a global network of VALs vs TNF- α

1
2
3
4 498 comparison. The network presented in Figure 9A shows at least three main clusters, dominated by
5
6 499 hsa-miR-6730-3p, hsa-miR-6730-5p, hsa-miR-6746-3p, hsa-miR-6746-5p. Likewise, lncRNA
7
8
9 500 smaller clusters are observed, formed by FTX, RP11-386G11.10, AC012668.2, AC005562.1,
10
11 501 CTD-2031P19.5 as central hubs. Moreover, the global network of enriched pathway interactions
12
13
14 502 of our omic layers (mRNAs, miRNAs, lncRNAs and proteins) was grouped and shown in Figure
15
16 503 9B-C, where individual clusters were not differentiated, but rather a centralized network. The
17
18
19 504 pathways with the highest degree of connections with other pathways into the network are
20
21 505 pathways in cancer, focal adhesion, thyroid hormone signaling pathway, RAS signaling, PI3K-
22
23
24 506 Akt signaling and Rap1 signaling.

25
26 507 Our next step was to identify common enriched pathways to mRNAs, miRNAs, lncRNAs and
27
28
29 508 proteins. As shown in the heatmap in Figure 10A, pathways specific to one, 2, or 3 omic analyses
30
31 509 (mRNA, miRNA, lncRNA) were identified but also a group of pathways, 30, have been identified
32
33 510 as common for all the 4 omics analyses (mRNA, miRNA, lncRNA and proteins). Among these
34
35
36 511 pathways are gap junction, regulation of actin cytoskeleton chemokine signaling pathway, PPAR
37
38 512 signaling, PI3K signaling, Ras signaling or focal adhesion (Figure 10A, side box). Figure 10B
39
40
41 513 provides an example of integration for the focal adhesion pathway showing the integrated analysis
42
43 514 of the four regulatory layers, that is mRNA, miRNA, lncRNA and protein regulation, with their
44
45
46 515 interactions, revealing how this pathway can be modulated by γ -valerolactones. Some genes
47
48 516 involved in focal adhesion are regulated by miRNAs and lncRNAs, such as Integrin beta (ITGB),
49
50
51 517 found in protein, mRNA and miRNA map and regulated by hsa-miR-6746-3p. Integrin-linked
52
53 518 protein kinase (ILK) found in the protein and lncRNA map and being regulated by RP11-
54
55 519 732A19.2. Phosphatase and tensin homolog (PTEN) is found in the miRNA map and regulated by
56
57
58 520 miR-6730-5p and miR-6730-3p. Protein kinase (PAK) protein is regulated by miR-6730-5p.

59
60
61
62
63
64
65

1
2
3
4
5
6
7
8
9
10
11
12
13
14
15
16
17
18
19
20
21
22
23
24
25
26
27
28
29
30
31
32
33
34
35
36
37
38
39
40
41
42
43
44
45
46
47
48
49
50
51
52
53
54
55
56
57
58
59
60
61
62
63
64
65

521 Taken together, this integrated multi-omic analysis suggests that genomic modifications induced
522 by γ -valerolactones highly impact pathways regulating endothelial cell function and permeability.

523

524 **4. Discussion**

525 The BBB plays an important role in brain health and is often compromised in disease. The BBB
526 is composed of BMECs and other cells such as astrocytes and matrix molecules that help regulate
527 the flow of immune cells and molecules into and out of the brain. Complex intercellular tight
528 junctions limit the passive diffusion of molecules into the brain [31]. Neuroinflammation and
529 mitochondrial dysfunction are common features of chronic neurodegenerative diseases of the
530 central nervous system. Both conditions can lead to increased oxidative stress by excessive release
531 of harmful reactive oxygen and nitrogen species, which further promote neuronal damage and
532 subsequent inflammation resulting in a feed-forward loop of neurodegeneration. The cytokine
533 TNF- α , a master regulator of the immune system, plays an important role in the propagation of
534 inflammation due to the activation and recruitment of immune cells via its receptor TNF receptor
535 1 (TNFR1). TNF- α may play a dual role in neurodegenerative disease, since stimulation via its
536 second receptor, TNFR2, is neuroprotective and promotes tissue regeneration [32]. However, it
537 has been reported that the levels of both TNFR1 and TNFR2 were significantly correlated with
538 amyloid- β oligomers (A β O) levels, considered as the most proximal neurotoxic species, in
539 amnesic mild cognitive impairment and mild AD patients [33]. TNF- α mediates double-stranded
540 RNA-dependent protein kinase (PKR)-dependent memory impairment and brain insulin receptor
541 substrate 1 inhibition induced by Alzheimer's A β O in mice and monkeys [34]. Natural
542 compounds, especially polyphenols, have proven capable of modifying different
543 neuropathological features, such as in AD. Special attention, in this context, has been given to

1
2
3
4
5
6
7
8
9
10
11
12
13
14
15
16
17
18
19
20
21
22
23
24
25
26
27
28
29
30
31
32
33
34
35
36
37
38
39
40
41
42
43
44
45
46
47
48
49
50
51
52
53
54
55
56
57
58
59
60
61
62
63
64
65

544 flavan-3-ols, polycyclic flavonoids that are particularly abundant in cocoa, tea, berries, red wine
545 and other plant-derived foods and beverages. Phenyl-valerolactones (PVL) are the major group of
546 circulating flavan-3-ol metabolites in humans [3]. A β O inhibition may indicate a mechanism by
547 which γ -valerolactones could inhibit inflammatory processes in neurodegenerative diseases and
548 subsequently protect endothelial integrity, however, the direct effect of γ -valerolactones on
549 HBMEC has not been elucidated.

550 In this study we assessed the effect of γ -valerolactones treatment on HBMEC cells on the inhibition
551 of TNF- α -generated stress *in vitro*, through the multi-omic data analysis that included mRNAs,
552 miRNAs, lncRNAs and proteins layers integration (**Figure 11**). We observed that TNF- α alone
553 exerted greater genomic modifications on transcript and protein modulation than treatment with
554 TNF- α + γ -valerolactones (VALs), which could indicate that the pro inflammatory effect of TNF-
555 α could be corrected by these metabolites. We performed an analysis of differential expression and
556 pathways associated for each omic data category individual and globally. After the treatment with
557 VALs, we assessed that miRNA targets-mapped pathways are more associated with cell signaling
558 and those protein-mapped pathways are more related with metabolism. However, when we
559 performed the omic integration analysis, we observed a strong association between cell adhesion
560 and permeability pathways, such as, focal adhesion, tight junction, gap junction, adherent junctions
561 with cell signaling pathways, such as, Rap1, PI3K-Akt, Wnt, and thyroid hormone signaling.
562 Signaling pathways such as Rap1, Wnt and PI3K-Akt, has been found to play a crucial role in the
563 maintenance of cell-cell regulation [35,36].

564 Our analysis allowed us to extract some key elements and their targets interactions in the
565 modulation of EC functions pathways. Here, we identified mRNAs, miRNAs, lncRNAs and
566 proteins involved in cell adhesion and permeability functions. miRNAs are short ncRNAs with a

1
2
3
4
5
6
7
8
9
10
11
12
13
14
15
16
17
18
19
20
21
22
23
24
25
26
27
28
29
30
31
32
33
34
35
36
37
38
39
40
41
42
43
44
45
46
47
48
49
50
51
52
53
54
55
56
57
58
59
60
61
62
63
64
65

length of 19–23 nucleotides. MiRNAs have two main functions: post-transcriptional gene regulation and RNA silencing. Consequently, the mRNAs are regulated by one or more mechanisms that include the inhibition of mRNA translation to proteins by ribosomes and by mRNA strand cleavage into two fragments and poly(A) tail shortening that results in mRNA disruption [37]. Clues about brain endothelial function modulated by miRNAs such as hsa-miR-146a-3p, hsa-miR-214-3p in the TNF- α group and hsa-miR-6746 and miR-6730-5p in the VALs group were obtained in our analysis. Deng S et al. (2017), showed that miR-146a was upregulated in lineage negative bone marrow cells in aged mice, which were enriched in endothelial progenitor cells (EPCs) [38]. Overexpression of miR-146a enhanced senescence and augmented apoptosis, suggesting that miR-146a inhibition improves the capacity of vascular repair in EPCs [38]. On the other hand, stimulation of primary Human Umbilical Vein Endothelial Cells (HUVECs) with lipopolysaccharide (LPS) promoted the production of miR-146a in replicative senescent HUVECs [39]. Since pro-inflammatory conditions, such as chronic heart failure, accelerated senescence of ECs, the increase of miR-146a in ECs might represent senescence-associated pro-inflammatory conditions in the vasculature. *In vitro*, TNF- α and IFN γ treatment of human cerebral microvascular endothelial cells (hCMEC/D3) led to upregulation of miR-146a, what agrees with our data [40]. On the other hand, miR-214, other miRNA found in TNF- α group is suggested as a biomarker to detect early stages of Parkinson's disease [41]. Hsa-miR-6746 is a miRNA found upregulated in VALs group, this miRNA has been studied in different contexts, but scarce information exists about its relationship with EC function. It would be interesting to extrapolate the epigenetic mechanisms attributed to this miRNA to study the function of brain ECs. In this regard, it has been reported that the splicing activator protein SRSF2 and the splicing inhibitor protein HNRNPD may be implicated in EC senescence. EC senescence

1
2
3
4
5
6
7
8
9
10
11
12
13
14
15
16
17
18
19
20
21
22
23
24
25
26
27
28
29
30
31
32
33
34
35
36
37
38
39
40
41
42
43
44
45
46
47
48
49
50
51
52
53
54
55
56
57
58
59
60
61
62
63
64
65

590 has also been associated with vascular dysfunction and increased vascular risk. Our observations
591 demonstrated that SRSF2 can be targeted by miR-6730-5p and miR-6746-5p, two miRNAs
592 differentially expressed in VALs group, which could indicate a VALs prevent EC dysfunction
593 mechanism.

594 LncRNAs are all ncRNAs larger than 200 nucleotides and are classified according to their
595 proximity to protein-coding genes as intergenic, intronic, bidirectional, sense, and antisense
596 lncRNAs. The main function of a signal lncRNA is to serve as a molecular signal to regulate
597 transcription in response to various stimuli [42]. LncRNAs show tissue-specific expression
598 patterns and are predominantly located in the nucleus rather than the cytoplasm. In fact, there are
599 several lines of evidence that suggest that lncRNAs are significantly more enriched in chromatin
600 than miRNAs [37]. In our analysis, we identified lncRNAs differentially expressed, such as FTX,
601 RP11-386G11.10, RP11-192H23.7, AC012668.2, AC005562.1 found in VALs group, and
602 searched their connections in brain EC function. For instance, five primes to Xist (FTX) is
603 downregulated in VALs group, and it was shown that overexpression of FTX inhibited apoptosis
604 in H2O2 treated cardiomyocyte and ischemia- reperfusion (I/R) injury mice model by negatively
605 regulating miR-29b-1-5p [43]. miR-29 is required for normal endothelial function in humans and
606 animal models and has therapeutic potential for cardiometabolic [44]. Therefore, downregulation
607 of FTX could contribute to upregulation of miR-29 and subsequently to an improvement in EC
608 function.

609 Mechanistically, peroxisome proliferator-activated receptor γ (PPAR γ) expression in human
610 hepatocellular carcinoma tissues and cell lines was positively correlated with lncRNA FTX [45].
611 PPAR γ overexpression in brain EC results in selective abrogation of inflammation-induced ICAM-
612 1 and VCAM-1 upregulation and subsequent adhesion and transmigration of T cells. Therefore, it

1
2
3
4
5
6
7
8
9
10
11
12
13
14
15
16
17
18
19
20
21
22
23
24
25
26
27
28
29
30
31
32
33
34
35
36
37
38
39
40
41
42
43
44
45
46
47
48
49
50
51
52
53
54
55
56
57
58
59
60
61
62
63
64
65

613 has been proposed that PPAR γ in brain EC may be exploited to target detrimental EC-T cell
614 interactions under inflammatory conditions [46]. Moreover, HIV-1 neuropathogenesis, enhanced
615 adhesion and migration of HIV-1 infected monocytes across the BBB were significantly reduced
616 when bovine brain microvascular endothelial cells (BMVEC) were treated with PPAR γ agonist.
617 These findings indicate that PPAR γ agonists could be a new approach for treatment of
618 neuroinflammation by preventing monocyte migration across the BBB [47]. FTX appears to be
619 related to PPAR γ , although FTX was down-regulated in our study, PPAR γ signaling was one of
620 the enriched pathways in our global enrichment analysis. Therefore, diverse mechanisms must
621 converge for PPAR γ to be activated in the VALs group.

622 Likewise, we identified TFs regulating our mRNA omic layer. NF- κ B, it was one of the
623 transcriptional factors found in our analysis, regulating some of the differentially expressed
624 transcripts. NF κ B activation initiates the canonical and non-conical pathways that promote
625 activation of TFs leading to inflammation, such as leukocyte adhesion molecules, cytokines, and
626 chemokines. However, flavonoids may modulate the expression of pro-inflammatory genes
627 leading to the attenuation of the inflammatory responses underlying various pathologies [48]. It
628 has been corroborated that small molecules, derived from dietary (poly)phenols may cross the
629 BBB, reach brain cells, modulate microglia-mediated inflammation and exert neuroprotective
630 effects, with potential for alleviation of neurodegenerative diseases. The (poly)phenol metabolites
631 attenuated neuro-inflammatory processes via regulation of nuclear factor (NF)- κ B translocation
632 into the nucleus and modulation of I κ B α (inhibitor of NF- κ B) levels [49]. Our in-silico docking
633 analysis also suggests that valerolactones metabolites present capacity to bind to this transcription
634 factor, binding that could affect its activity and consequently expression of related genes. This
635 analysis also suggested that the studied valerolactone metabolites present potential binding

1
2
3
4
5
6
7
8
9
10
11
12
13
14
15
16
17
18
19
20
21
22
23
24
25
26
27
28
29
30
31
32
33
34
35
36
37
38
39
40
41
42
43
44
45
46
47
48
49
50
51
52
53
54
55
56
57
58
59
60
61
62
63
64
65

636 capacity to different transcription factors. Earlier studies have suggested that epicatechin
637 secondary metabolites can bind to these cell signaling proteins [19] but it is first to suggest such
638 interaction for gut metabolites.

639 By omic layers integration, our analysis allowed us to find relationships between HBMEC and
640 focal adhesion pathways. We were able to identify components mapped to the focal adhesion
641 network, which were differentially regulated in our study (Figure 10). For instance, alpha integrin
642 (ITGA) and ITGB and their relationship with Platelet endothelial cell adhesion molecule
643 (PECAM1-1). PECAM-1 is critically involved in regulating BBB permeability and although not
644 required for T-cell diapedesis itself, its presence or absence influences the cellular route of T-cell
645 diapedesis across the BBB [50]. In ECs, this molecule controls junctional and adhesive properties.
646 It is reported that although in physiological conditions, PECAM-1 supports the endothelial barrier
647 function, in inflammation that is observed in vessels affected by atherosclerosis, the function of
648 PECAM-1 is impaired, an event that leads to increased adhesion of neutrophils and other
649 leukocytes to ECs, decreased vascular integrity, and higher leukocyte transmigration to the intima
650 media. PECAM-1 contains six extracellular Ig-like domains that mediate the attraction and
651 adhesion of leukocytes to EC, for example by enhancing eosinophil adhesion to IL-4-stimulated
652 HUVECs in an $\alpha 4\beta 1$ integrin-dependent manner [51]. Therefore, searching for mechanisms that
653 mediate PECAM-1 interactions with beta or alpha integrins is of importance. Hsa-miR-6746-3p
654 and hsa-miR-6730-5p were two differentially regulated miRNAs in the VALs group and whose
655 targets include ITGA and ITGB. In conditions of stress, such as TGF- β stimulus, the inhibition of
656 these two integrins, could prevent leukocyte transendothelial migration (TEM) under
657 inflammatory conditions.

1
2
3
4
5
6
7
8
9
10
11
12
13
14
15
16
17
18
19
20
21
22
23
24
25
26
27
28
29
30
31
32
33
34
35
36
37
38
39
40
41
42
43
44
45
46
47
48
49
50
51
52
53
54
55
56
57
58
59
60
61
62
63
64
65

658 Another possible mechanism of VALs function against TNF- α inflammation could be mediated
659 by Integrin-linked kinase (ILK). An ILK knockdown significantly decreased β 1-integrin
660 expression by 24 h after transfection of confluent primary cerebral microvessel endothelial cells
661 that was accompanied by a significant decrease in claudin-5 expression, and a small significant
662 change in F-actin. ILK is essential for EC survival, vascular development, and cell integrin–matrix
663 interactions in mice. Yet, there is little information about the role(s) of ILK in tight junction protein
664 expression or permeability in the CNS in inflammatory processes [52]. In a study aimed to explore
665 the mechanism of the function of TGF- β signaling in dermal lymphatic endothelial cells (LECs)
666 epithelial–mesenchymal transition (EMT) it was found that TGF- β treatment increased the
667 expression level of ILK Human lens epithelial cells (HLEC-h3), promoted migration of HLEC-h3
668 cells, increased the expression level of E-cadherin protein, and decreased the expression level of
669 α -SMA protein, playing an important role in fibrogenesis. However, treatment with ILK siRNA,
670 ILK inhibitor, and NF- κ B inhibitor reversed the effects of TGF- β on HLEC-h3 cells [53]. In our
671 study, ILK was a target of the lncRNA RP11-732A19.2, differentially expressed in our VALs
672 group which could indicate a possible mechanism, by which γ -valerolactones inhibit the
673 inflammatory process of TNF- α . Preventing neuronal damage and neuronal death have a huge
674 clinical benefit. Flavonoids are key compounds for the development of a new generation of
675 therapeutic agents that could be clinically effective in treating neurodegenerative diseases. Regular
676 consumption of flavonoids has been associated with a reduced risk of neurodegenerative diseases
677 (Solanki et al, 2015). The molecular targets identified in our study will supply the basis for the
678 development of future therapeutic targets.

679

1
2
3
4
5
6
7
8
9
10
11
12
13
14
15
16
17
18
19
20
21
22
23
24
25
26
27
28
29
30
31
32
33
34
35
36
37
38
39
40
41
42
43
44
45
46
47
48
49
50
51
52
53
54
55
56
57
58
59
60
61
62
63
64
65

680 Figure legends

681 Figure 1. TNF- α modulates the expression of mRNAs, miRNAs, lncRNAs and proteins in
682 human brain microvascular endothelial cells. HBMEC cells induced under stress by 4h-
incubation with TNF- α were used in microarray analysis and proteomic analysis to determine the
differential expression of transcripts and proteins between groups. A) Manhattan plot of total
transcripts, 983 transcripts positioned above the line were considered differentially expressed. B)
Histogram of the number of differentially expressed mRNAs, miRNAs, lncRNAs and proteins. C)
Venn diagram to indicate the relations between the number of mRNAs, miRNAs targets, lncRNA
targets and proteins differentially expressed. D) Global network of interactions modulated by TNF-
 α treatment in HBMEC cells. The total interactions between mRNAs, miRNAs and targets,
lncRNAs and targets and protein-protein interactions were used to build a network with Cytoscape
software. Nodes colored labels. Red-lncRNAs, blue marine-miRNAs, green-miRNAs targets and
mRNAs DE, pink-lncRNA targets and mRNA DE, yellow-lncRNA and miRNA targets and
mRNA no DE, purple-mRNAs DE, melon-proteins and mRNA DE, clear purple -proteins and
mRNAs DE and regulated by miRNAs or lncRNAs, blue clair-proteins and mRNAs no DE. DE =
differentially expressed. E) Zoom network of interactions between the components of each omic
layer and also corresponding to differentially expressed mRNAs. Nodes colored labels. Red-
lncRNAs, blue marine-miRNAs, green-miRNA targets, pink-lncRNA targets, yellow-lncRNA and
miRNA targets, melon-proteins, clear purple-proteins regulated by miRNAs and lncRNAs.

700 Figure 2. Enriched pathways of differentially expressed transcripts and proteins of human
701 brain microvascular endothelial cells treated with TNF- α vs control. Differentially expressed
transcripts and proteins between study groups were used in a GeneTrail analysis to obtain the list

1
2
3
4 703 of enriched pathways. Subsequently, a set of genes involved in KEGG endothelial pathway
5
6 704 functions was used to map against our differentially expressed transcripts and proteins. A)
7
8
9 705 Histogram that shows the number of transcripts and proteins mapped to the enriched pathways.
10
11 706 The blue bars represent the enriched pathways of mRNAs, the green bars of miRNAs, the yellow
12
13
14 707 bars of lncRNAs and the red bars of proteins. B) Network of interactions between mRNAs,
15
16 708 miRNAs and targets, lncRNAs and targets, protein-protein interactions related to a set of genes
17
18
19 709 involved in endothelial cell functions. Node colored labels. Red-lncRNAs, blue marine-miRNAs,
20
21 710 green-miRNAs targets and mRNAs DE, yellow-lncRNA and miRNA targets and mRNA no DE,
22
23
24 711 melon-proteins and mRNA DE, clear purple-proteins and mRNAs DE and regulated by miRNAs
25
26 712 or lncRNAs, blue clair-proteins and mRNAs no DE, black-miRNA and lncRNA target and mRNA
27
28
29 713 DE, white-miRNA target or lncRNA target and mRNA no DE. DE= differentially expressed.
30

31 714
32
33
34 715 **Figure 3. Genomic modifications induced by γ -valerolactones treatment in human brain**
35
36 716 **microvascular endothelial cells.** HBMEC cells exposed to the mixture of gut metabolites (γ -
37
38
39 717 valerolactones) for 20h and induced under stress by 4h-incubation with TNF- α were used in
40
41 718 microarray analysis and proteomic analysis to determine the differential expression of transcripts
42
43
44 719 and proteins between groups, respectively. A) A 3D Principal component analysis (PCA) plot of
45
46 720 the data that characterizes the trends exhibited by the expression profiles of HBMEC cell no treated
47
48
49 721 with TNF- α (control, blue), cells treated with TNF- α (TNF- α , red) and cells treated with VALs
50
51 722 + TNF- α (VALs, purple). Each dot represents a sample and each color represents the type of the
52
53
54 723 sample. B) Histogram of the number of differentially expressed mRNAs, miRNAs, lncRNAs and
55
56 724 proteins. C) Manhattan plot of total transcripts, 211 transcripts positioned above the line were
57
58
59 725 considered differentially expressed. D) Heatmap shows transcript abundance (expression level) in
60
61
62
63
64
65

1
2
3
4
5
6
7
8
9
10
11
12
13
14
15
16
17
18
19
20
21
22
23
24
25
26
27
28
29
30
31
32
33
34
35
36
37
38
39
40
41
42
43
44
45
46
47
48
49
50
51
52
53
54
55
56
57
58
59
60
61
62
63
64
65

726 each group. In red are upregulated classes of genes (>2-fold standard deviation); in green are
727 downregulated classes of genes (<2-fold standard deviation). Classes were grouped by a pattern
728 of transcription, genes that are upregulated in both tissues; genes that are differentially expressed,
729 genes that are downregulated in both tissues.

730

731 **Figure 4. Enriched pathways of protein-coding genes differentially expressed in human brain**
732 **microvascular endothelial cells treated with γ -valerolactones.** Differentially expressed
733 protein-coding genes between VALs and TNF- α groups were used in a GeneTrail analysis to
734 obtain the list of enriched pathways. A) Histogram that shows the number of genes mapped to the
735 enriched pathways classified in cell adhesion and permeability, cell signaling, cell metabolism and
736 other pathways. B) Pathway interactions network built in Cytoscape software to show the
737 connections (edges) between enriched pathways (nodes) by differentially expressed protein-
738 coding genes.

739

740 **Figure 5. MiRNAs expression mediated by γ -valerolactones treatment in human brain**
741 **microvascular endothelial cells and their relation with endothelial cell functions.** HBMEC
742 cells exposed to the mixture of gut metabolites (γ -valerolactones) for 20h and induced under stress
743 by 4h-incubation with TNF- α were used in microarray analysis to determine the differential
744 expression of miRNAs between groups. Subsequently, the miRNAs targets were obtained from an
745 analysis of databases (miRTarbase, TargetScan and miRDB). An enrichment pathway analysis of
746 miRNAs targets in GeneTrail was also performed. A) Network of miRNAs differentially expressed
747 and their targets. Network built in Cytoscape software. Hubs network components are highlighted
748 by red squares. B) Histogram that shows the number of genes mapped to the enriched pathways

1
2
3
4
5
6
7
8
9
10
11
12
13
14
15
16
17
18
19
20
21
22
23
24
25
26
27
28
29
30
31
32
33
34
35
36
37
38
39
40
41
42
43
44
45
46
47
48
49
50
51
52
53
54
55
56
57
58
59
60
61
62
63
64
65

749 classified as endothelial cells related (blue), cell signaling (green), cell metabolism (yellow) and
750 other pathways (red).

751
Figure 6. LncRNAs expression mediated by γ -valerolactones treatment in human brain
microvascular endothelial cells and their relation with endothelial cell functions. HBMEC
752 cells exposed to the mixture of gut metabolites (γ -valerolactones) for 20h and cells induced under
753 stress by 4h-incubation with TNF- α were used in microarray analysis to determine the differential
754 expression of lncRNAs between groups. Subsequently, the lncRNAs targets were obtained from
755 an analysis of databases (RNARNA, LncRRIsearch). An enrichment pathway analysis of miRNAs
756 targets in GeneTrail was also performed. A) Network of lncRNAs differentially expressed and
757 their targets. Network built in Cytoscape software. Hubs network components are highlighted by
758 red squares. B) lncRNA targets were overrepresented by genes coding for KEGG, Biocarta and
759 Wiki modules associated with endothelial cell related, cellular metabolism, cell signaling and other
760 pathways. C) lncRNA-enriched pathway interactions network. Pathway interactions network built
761 in Cytoscape software to show the connections (edges) between enriched pathways (nodes) by
762 lncRNAs differentially expressed. Hubs network components are highlighted by yellow circles.

765
Figure 7. Protein expression mediated by γ -valerolactones treatment in human brain
microvascular endothelial cells and their relation with endothelial cell functions. HBMEC
766 cells exposed to the mixture of gut metabolites (γ -valerolactones) for 20h and cells induced under
767 stress by 4h-incubation with TNF- α were used in shotgun proteomic analysis to determine the
768 differential expression of proteins between groups. An enrichment pathway analysis of miRNAs
769 targets in GeneTrail was also performed. A) Proteins differentially expressed mapped onto KEGG,

1
2
3
4
5
6
7
8
9
10
11
12
13
14
15
16
17
18
19
20
21
22
23
24
25
26
27
28
29
30
31
32
33
34
35
36
37
38
39
40
41
42
43
44
45
46
47
48
49
50
51
52
53
54
55
56
57
58
59
60
61
62
63
64
65

772 Biocarta and Wikipathways modules associated with endothelial cell function, cell metabolism,
773 cell signaling pathways and others. B) Proteins-enriched pathway interactions network, pathway
774 interactions network built in Cytoscape software to show the connections (edges) between
775 enriched pathways (nodes) by proteins differentially expressed. Hubs network components are
776 highlighted by yellow circles.

777
778 Figure 8. Transcription factors potentially involved in the nutrigenomic modifications
779 induces by γ -valerolactones and their *in-silico* interaction with RelA subunit of NF- κ B. A)
780 List of potential transcription factors identified using bioinformatic analysis. Binding mode
781 obtained by computational docking for: (B) 5-(4'-Hydroxyphenyl)- γ -valerolactone-3'-sulfate and
782 (C) 5-(4'-Hydroxyphenyl)- γ -valerolactone-3'-O-glucuronide.

783
784 Figure 9. Global network of interactions modulated by γ -valerolactones treatment in human
785 brain microvascular endothelial cells and their relation with endothelial function pathways.
786 A) The total interactions between mRNAs, miRNAs and targets, lncRNAs and targets and protein-
787 protein interactions were used to build a network with Cytoscape software. Nodes colored labels.
788 Red-lncRNAs, blue marine-miRNAs, green-miRNAs targets and mRNAs DE, pink-lncRNA
789 targets and mRNA DE, yellow-lncRNA and miRNA targets and mRNA no DE, purple-mRNAs
790 DE, blue clair-proteins and mRNAs no DE, black-miRNA and lncRNA target and mRNA DE,
791 clair green-proteins and mRNA no DE and regulated by miRNA or lncRNA, olive-TFs, white-
792 components not belonging to any of the previous color categories. DE = differentially expressed.
793 Hubs network components are highlited by bigger squares. B) mRNA, miRNA targets, lncRNA
794 targets and proteins were used to perform a global GeneTrial enrichment analysis and obtained the

1
2
3
4 795 pathways related. A pathway-connections network was built in Cytoscape. Node colored labels
5
6 796 represent the omic layers (mRNA, miRNA targets, mRNA targets, proteins or combinations) from
7
8
9 797 which the pathways were enriched. Yellow-miRNA, green-proteins, pink-
10
11 mRNA+lncRNA+miRNA, blue marine-miRNA+proteins, clair blue-mRNA+miRNAs, clair
12 798 purple-lncRNA+miRNA, red-mRNA+miRNA+lncRNA+proteins, melon-
13
14 799 lncRNA+miRNA+proteins, clair green-mRNA+miRNA+proteins. C) Small network of focal
15
16 800 adhesion components and regulated by miRNAs and lncRNAs differentially expressed in our
17
18 801 VALs vs TNF- α groups comparison.
19
20
21 802
22
23

24 803
25
26
27 804 **Figure 10. Integration of differentially expressed mRNAs, microRNA target gene, lncRNA**
28
29 805 **target gene and protein modulating focal adhesion function in human brain microvascular**
30
31 806 **endothelial cells treated with γ -valerolactones and stressed with TNF- α .** A) Heatmap of
32
33 807 differentially expressed gene pathways, miRNA target gene pathways, lncRNA gene pathways
34
35 808 and protein pathways. Comparisons of pathways between biological categories identified a group
36
37 809 of pathways in common including chemokine signaling pathway, cytokine cytokine receptor, focal
38
39 810 adhesion, gap junction, FOXO signaling, fatty acid metabolism and pathways that regulate
40
41 811 endothelial cell interaction and permeability. B) A representative integrated analysis of
42
43 812 differentially expressed genes and proteins, and target genes of differentially expressed miRNAs,
44
45 813 lncRNA is shown for Focal adhesion. Yellow= differentially expressed genes; Red= target genes
46
47 814 of differentially expressed miRNAs, Green=target genes of differentially expressed lncRNAs,
48
49 815 Blue= differentially expressed proteins. Color gradations= genes identified in both omic maps.
50
51
52
53
54
55

56 816
57
58
59 817
60
61
62
63
64
65

1
2
3
4
5
6
7
8
9
10
11
12
13
14
15
16
17
18
19
20
21
22
23
24
25
26
27
28
29
30
31
32
33
34
35
36
37
38
39
40
41
42
43
44
45
46
47
48
49
50
51
52
53
54
55
56
57
58
59
60
61
62
63
64
65

818 Supplemental figure legends

819

820 Supplemental Figure 1. Chemical structures of microbiota epicatechin metabolites.

821

822 Supplemental Figure 2. miRNA-enriched pathway interactions network. Pathway interactions
network built in Cytoscape software to show the connections (edges) between enriched pathways
(nodes) by miRNAs differentially expressed.

825

**826 Supplemental Figure 3. Venn diagrams of mRNAs, miRNAs targets, lncRNAs targets,
827 proteins and pathways related in human brain microvascular endothelial cells- γ -
828 valerolactone treatment cell.** A) Venn diagram indicates the relationships between the number
of mRNAs, miRNAs targets, lncRNA targets and proteins differentially expressed. B) Venn
diagram indicates the relationships between the number of enriched pathways-mRNAs, miRNAs
targets, lncRNA targets and proteins differentially expressed.

832

833 Supplemental table legends

834

**835 Supplemental Table 1. Effect of the γ -Valerolactones treatment on the expression of protein
836 coding genes in human brain microvascular endothelial cells.**

837

**838 Supplemental Table 2. Effect of the γ -Valerolactones treatment on the expression of miRNAs
839 in human brain microvascular endothelial cells.**

1
2
3
4
5
6
7
8
9
10
11
12
13
14
15
16
17
18
19
20
21
22
23
24
25
26
27
28
29
30
31
32
33
34
35
36
37
38
39
40
41
42
43
44
45
46
47
48
49
50
51
52
53
54
55
56
57
58
59
60
61
62
63
64
65

840

841 **Supplemental Table 3. Effect of the γ -Valerolactones treatment on the expression of lncRNAs**
842 **in human brain microvascular endothelial cells.**

843

844 **Supplemental Table 4. Effect of the γ -Valerolactones treatment on the expression of proteins**
845 **in HBMEC cells.**

846

847

848

849

850

1
2
3
4
5
6
7
8
9
10
11
12
13
14
15
16
17
18
19
20
21
22
23
24
25
26
27
28
29
30
31
32
33
34
35
36
37
38
39
40
41
42
43
44
45
46
47
48
49
50
51
52
53
54
55
56
57
58
59
60
61
62
63
64
65

851 Competing Interests

852 Dragan Milenkovic initiated the study that was partially funded through an unrestricted research
853 grant that he received from Mars Inc. Mars, Inc. also provided the epicatechin metabolites used in
854 this study. H.S. is employed by Mars Inc., a company engaged in flavanol research and flavanol-
855 related commercial activities.

856

857 The authors' roles

858 KF, SN and DM performed bioinformatic analyses and wrote the manuscript; SN and DM
859 performed microarray analysis; DM designed the research and had primary responsibility for final
860 content; All authors participated in the interpretation of the data and also read and approved the
861 final manuscript.

862

863

864 Acknowledgement

865 KF received fellowship from Auvergne-Rhône-Alpes region as part of the AUDACE project
866 ICARES (Identification and Characterization of Non-coding RNAs Under Stress Conditions)
867 supported by CPER2017; projet number 17 011085 01.

868

869

870

871

872

873

1
2
3
4
5
6
7
8
9
10
11
12
13
14
15
16
17
18
19
20
21
22
23
24
25
26
27
28
29
30
31
32
33
34
35
36
37
38
39
40
41
42
43
44
45
46
47
48
49
50
51
52
53
54
55
56
57
58
59
60
61
62
63
64
65

874 **References**

875

876 1. Vogiatzoglou A, Mulligan AA, Bhaniani A, Lentjes MAH, McTaggart A, Luben RN, et al.

877 Associations between flavan-3-ol intake and CVD risk in the Norfolk cohort of the European

878 Prospective Investigation into Cancer (EPIC-Norfolk). *Free Radic Biol Med* [Internet].

879 2015;84:1–10. Available from: <http://www.ncbi.nlm.nih.gov/pubmed/25795512>

880 2. Crozier A, Jaganath IB, Clifford MN. Dietary phenolics: chemistry, bioavailability and effects

881 on health. *Nat Prod Rep* [Internet]. 2009;26:1001–43. Available from:

882 <http://www.ncbi.nlm.nih.gov/pubmed/19636448>

883 3. Ottaviani JI, Borges G, Momma TY, Spencer JP, Keen CL, Crozier A, et al. The metabolome

884 of [2-(14)C](–)-epicatechin in humans: implications for the assessment of efficacy, safety, and

885 mechanisms of action of polyphenolic bioactives. *Sci Rep* [Internet]. 2016;6:29034. Available

886 from: <http://www.ncbi.nlm.nih.gov/pubmed/27363516>

887 4. Mena P, Bresciani L, Brindani N, Ludwig IA, Pereira-Caro G, Angelino D, et al. Phenyl-

888 gamma-valerolactones and phenylvaleric acids, the main colonic metabolites of flavan-3-ols:

889 synthesis, analysis, bioavailability, and bioactivity. *Nat Prod Rep* [Internet]. 2019;36:714–52.

890 Available from: <http://www.ncbi.nlm.nih.gov/pubmed/30468210>

891 5. Schroeter H, Heiss C, Balzer J, Kleinbongard P, Keen CL, Hollenberg NK, et al. (–)-

892 Epicatechin mediates beneficial effects of flavanol-rich cocoa on vascular function in humans.

893 *Proc Natl Acad Sci U S A*. 2006;103:1024–9.

894 6. Desch S, Schmidt J, Kobler D, Sonnabend M, Eitel I, Sareban M, et al. Effect of cocoa

895 products on blood pressure: systematic review and meta-analysis. *Am J Hypertens* [Internet].

896 2010;23:97–103. Available from: <http://www.ncbi.nlm.nih.gov/pubmed/19910929>

1
2
3
4
5
6
7
8
9
10
11
12
13
14
15
16
17
18
19
20
21
22
23
24
25
26
27
28
29
30
31
32
33
34
35
36
37
38
39
40
41
42
43
44
45
46
47
48
49
50
51
52
53
54
55
56
57
58
59
60
61
62
63
64
65

897 7. Nation DA, Sweeney MD, Montagne A, Sagare AP, D’Orazio LM, Pachicano M, et al.
898 Blood–brain barrier breakdown is an early biomarker of human cognitive dysfunction. *Nat Med*
899 [Internet]. Springer US; 2019;25:270–6. Available from: [http://dx.doi.org/10.1038/s41591-018-](http://dx.doi.org/10.1038/s41591-018-0297-y)
900 0297-y

901 8. Tarantini S, Tran CHT, Gordon GR, Ungvari Z, Csiszar A. Impaired neurovascular coupling
902 in aging and Alzheimer’s disease: Contribution of astrocyte dysfunction and endothelial
903 impairment to cognitive decline. *Exp Gerontol* [Internet]. 2017;94:52–8. Available from:
904 <http://www.ncbi.nlm.nih.gov/pubmed/27845201>

905 9. Wang J, Varghese M, Ono K, Yamada M, Levine S, Tzavaras N, et al. Cocoa extracts reduce
906 oligomerization of amyloid-beta: implications for cognitive improvement in Alzheimer’s disease.
907 *J Alzheimers Dis* [Internet]. 2014;41:643–50. Available from:
908 <http://www.ncbi.nlm.nih.gov/pubmed/24957018>

909 10. Nehlig A. The neuroprotective effects of cocoa flavanol and its influence on cognitive
910 performance. *Br J Clin Pharmacol* [Internet]. 2013;75:716–27. Available from:
911 <http://www.ncbi.nlm.nih.gov/pubmed/22775434>

912 11. Sokolov AN, Pavlova MA, Klosterhalfen S, Enck P. Chocolate and the brain:
913 neurobiological impact of cocoa flavanols on cognition and behavior. *Neurosci Biobehav Rev*
914 [Internet]. 2013;37:2445–53. Available from: <http://www.ncbi.nlm.nih.gov/pubmed/23810791>

915 12. Barrera-Reyes PK, de Lara JC, Gonzalez-Soto M, Tejero ME. Effects of Cocoa-Derived
916 Polyphenols on Cognitive Function in Humans. Systematic Review and Analysis of
917 Methodological Aspects. *Plant Foods Hum Nutr* [Internet]. 2020;75:1–11. Available from:
918 <http://www.ncbi.nlm.nih.gov/pubmed/31933112>

919 13. Lamport DJ, Pal D, Moutsiana C, Field DT, Williams CM, Spencer JP, et al. The effect of

1
2
3
4
5
6
7
8
9
10
11
12
13
14
15
16
17
18
19
20
21
22
23
24
25
26
27
28
29
30
31
32
33
34
35
36
37
38
39
40
41
42
43
44
45
46
47
48
49
50
51
52
53
54
55
56
57
58
59
60
61
62
63
64
65

920 flavanol-rich cocoa on cerebral perfusion in healthy older adults during conscious resting state: a
921 placebo controlled, crossover, acute trial. *Psychopharmacol* [Internet]. 2015;232:3227–34.
922 Available from: <http://www.ncbi.nlm.nih.gov/pubmed/26047963>

923 14. Brickman AM, Khan UA, Provenzano FA, Yeung LK, Suzuki W, Schroeter H, et al.
924 Enhancing dentate gyrus function with dietary flavanols improves cognition in older adults. *Nat*
925 *Neurosci* [Internet]. 2014;17:1798–803. Available from:
926 <http://www.ncbi.nlm.nih.gov/pubmed/25344629>

927 15. Palmer AM. The role of the blood brain barrier in neurodegenerative disorders and their
928 treatment. *J Alzheimer’s Dis*. 2011;24:643–56.

929 16. Montagne A, Barnes SR, Sweeney MD, Halliday MR, Sagare AP, Zhao Z, et al. Blood-Brain
930 barrier breakdown in the aging human hippocampus. *Neuron*. 2015;
931 17. Sweeney MD, Sagare AP, Zlokovic B V. Blood-brain barrier breakdown in Alzheimer
932 disease and other neurodegenerative disorders. *Nat Rev Neurol* [Internet]. Nature Publishing
933 Group; 2018;14:133–50. Available from: <http://dx.doi.org/10.1038/nrneurol.2017.188>

934 18. Claude S, Boby C, Rodriguez-Mateos A, Spencer JPE, Gérard N, Morand C, et al. Flavanol
935 metabolites reduce monocyte adhesion to endothelial cells through modulation of expression of
936 genes via p38-MAPK and p65-Nf-kB pathways. *Mol Nutr Food Res*. 2014;58.

937 19. Milenkovic D, Berghe W Vanden, Morand C, Claude S, van de Sandt A, Gorressen S, et al.
938 A systems biology network analysis of nutri(epi)genomic changes in endothelial cells exposed to
939 epicatechin metabolites. *Sci Rep*. 2018;8:1–17.

940 20. Karim N, Durbin-Johnson B, Rocke DM, Salemi M, Phinney BS, Naeem M, et al. Proteomic
941 manifestations of genetic defects in autosomal recessive congenital ichthyosis. *J Proteomics*
942 [Internet]. 2019;201:104–9. Available from: <http://www.ncbi.nlm.nih.gov/pubmed/30978464>

1
2
3
4
5
6
7
8
9
10
11
12
13
14
15
16
17
18
19
20
21
22
23
24
25
26
27
28
29
30
31
32
33
34
35
36
37
38
39
40
41
42
43
44
45
46
47
48
49
50
51
52
53
54
55
56
57
58
59
60
61
62
63
64
65

943 21. Hsu SD, Lin FM, Wu WY, Liang C, Huang WC, Chan WL, et al. miRTarBase: a database
944 curates experimentally validated microRNA-target interactions. *Nucleic Acids Res* [Internet].
945 2011;39:D163-9. Available from: <http://www.ncbi.nlm.nih.gov/pubmed/21071411>

946 22. Chen Y, Wang X. miRDB: an online database for prediction of functional microRNA targets.
947 *Nucleic Acids Res* [Internet]. 2020;48:D127–31. Available from:
948 <http://www.ncbi.nlm.nih.gov/pubmed/31504780>

949 23. Agarwal V, Bell GW, Nam JW, Bartel DP. Predicting effective microRNA target sites in
950 mammalian mRNAs. *Elife* [Internet]. 2015;4. Available from:
951 <http://www.ncbi.nlm.nih.gov/pubmed/26267216>

952 24. Fukunaga T, Iwakiri J, Ono Y, Hamada M. LncRRsearch: A Web Server for lncRNA-RNA
953 Interaction Prediction Integrated With Tissue-Specific Expression and Subcellular Localization
954 Data. *Front Genet* [Internet]. 2019;10:462. Available from:
955 <http://www.ncbi.nlm.nih.gov/pubmed/31191601>

956 25. Szklarczyk D, Morris JH, Cook H, Kuhn M, Wyder S, Simonovic M, et al. The STRING
957 database in 2017: quality-controlled protein-protein association networks, made broadly
958 accessible. *Nucleic Acids Res* [Internet]. 2017;45:D362–8. Available from:
959 <http://www.ncbi.nlm.nih.gov/pubmed/27924014>

960 26. Kuleshov M V, Jones MR, Rouillard AD, Fernandez NF, Duan Q, Wang Z, et al. Enrichr: a
961 comprehensive gene set enrichment analysis web server 2016 update. *Nucleic Acids Res*
962 [Internet]. 2016;44:W90-7. Available from: <http://www.ncbi.nlm.nih.gov/pubmed/27141961>

963 27. Sanchez-Linares I, Perez-Sanchez H, Cecilia JM, Garcia JM. High-Throughput parallel blind
964 Virtual Screening using BINDSURF. *BMC Bioinformatics* [Internet]. 2012;13 Suppl 14:S13.
965 Available from: <http://www.ncbi.nlm.nih.gov/pubmed/23095663>

1
2
3
4
5
6
7
8
9
10
11
12
13
14
15
16
17
18
19
20
21
22
23
24
25
26
27
28
29
30
31
32
33
34
35
36
37
38
39
40
41
42
43
44
45
46
47
48
49
50
51
52
53
54
55
56
57
58
59
60
61
62
63
64
65

28. Backes C, Keller A, Kuentzer J, Kneissl B, Comtesse N, Elnakady YA, et al. GeneTrail--
advanced gene set enrichment analysis. *Nucleic Acids Res [Internet]*. 2007;35:W186-92.
Available from: <http://www.ncbi.nlm.nih.gov/pubmed/17526521>

29. Su G, Morris JH, Demchak B, Bader GD. Biological network exploration with Cytoscape 3.
Curr Protoc Bioinforma [Internet]. 2014;47:8 13 1-24. Available from:
<http://www.ncbi.nlm.nih.gov/pubmed/25199793>

30. Kanehisa M, Goto S. KEGG: kyoto encyclopedia of genes and genomes. *Nucleic Acids Res*
[Internet]. 2000;28:27–30. Available from: <http://www.ncbi.nlm.nih.gov/pubmed/10592173>

31. Lippmann ES, Azarin SM, Kay JE, Nessler RA, Wilson HK, Al-Ahmad A, et al. Derivation
of blood-brain barrier endothelial cells from human pluripotent stem cells. *Nat Biotechnol*
[Internet]. 2012;30:783–91. Available from: <http://www.ncbi.nlm.nih.gov/pubmed/22729031>

32. Fischer R, Maier O. Interrelation of oxidative stress and inflammation in neurodegenerative
disease: role of TNF. *Oxid Med Cell Longev [Internet]*. 2015;2015:610813. Available from:
<http://www.ncbi.nlm.nih.gov/pubmed/25834699>

33. Zheng D, Sun H, Dong X, Liu B, Xu Y, Chen S, et al. Executive dysfunction and gray matter
atrophy in amnesic mild cognitive impairment. *Neurobiol Aging [Internet]*. 2014;35:548–55.
Available from: <http://www.ncbi.nlm.nih.gov/pubmed/24119547>

34. Lourenco M V, Clarke JR, Frozza RL, Bomfim TR, Forny-Germano L, Batista AF, et al.
TNF-alpha mediates PKR-dependent memory impairment and brain IRS-1 inhibition induced by
Alzheimer's beta-amyloid oligomers in mice and monkeys. *Cell Metab [Internet]*. 2013;18:831–
839. Available from: <http://www.ncbi.nlm.nih.gov/pubmed/24315369>

35. Shah J, Rouaud F, Guerrera D, Vasileva E, Popov LM, Kelley WL, et al. A Dock-and-Lock
Mechanism Clusters ADAM10 at Cell-Cell Junctions to Promote alpha-Toxin Cytotoxicity. *Cell*

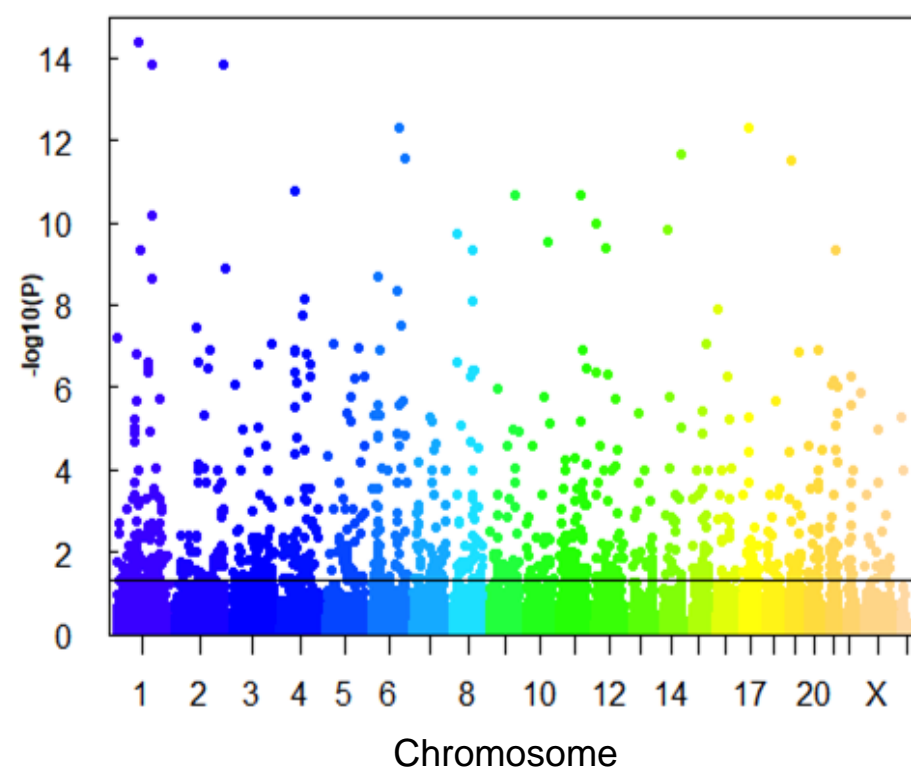
1
2
3
4 989 Rep [Internet]. 2018;25:2132-2147 e7. Available from:
5
6
7 990 <http://www.ncbi.nlm.nih.gov/pubmed/30463011>
8
9 991 36. Jasaitis A, Estevez M, Heysch J, Ladoux B, Dufour S. E-cadherin-dependent stimulation of
10
11 992 traction force at focal adhesions via the Src and PI3K signaling pathways. *Biophys J* [Internet].
12
13 993 2012;103:175–84. Available from: <http://www.ncbi.nlm.nih.gov/pubmed/22853894>
14
15
16 994 37. Hernandez-Romero IA, Guerra-Calderas L, Salgado-Albarran M, Maldonado-Huerta T,
17
18
19 995 Soto-Reyes E. The Regulatory Roles of Non-coding RNAs in Angiogenesis and
20
21 996 Neovascularization From an Epigenetic Perspective. *Front Oncol* [Internet]. 2019;9:1091.
22
23 997 Available from: <http://www.ncbi.nlm.nih.gov/pubmed/31709179>
24
25
26 998 38. Deng S, Wang H, Jia C, Zhu S, Chu X, Ma Q, et al. MicroRNA-146a Induces Lineage-
27
28
29 999 Negative Bone Marrow Cell Apoptosis and Senescence by Targeting Polo-Like Kinase 2
30
31 1000 Expression. *Arter Thromb Vasc Biol* [Internet]. 2017;37:280–90. Available from:
32
33 1001 <http://www.ncbi.nlm.nih.gov/pubmed/27908889>
34
35
36 1002 39. Olivieri F, Lazzarini R, Recchioni R, Marcheselli F, Rippo MR, Di Nuzzo S, et al. MiR-146a
37
38 1003 as marker of senescence-associated pro-inflammatory status in cells involved in vascular
39
40
41 1004 remodelling. *Age* [Internet]. 2013;35:1157–72. Available from:
42
43 1005 <http://www.ncbi.nlm.nih.gov/pubmed/22692818>
44
45
46 1006 40. Wu D, Cerutti C, Lopez-Ramirez MA, Pryce G, King-Robson J, Simpson JE, et al. Brain
47
48 1007 endothelial miR-146a negatively modulates T-cell adhesion through repressing multiple targets
49
50
51 1008 to inhibit NF-kappaB activation. *J Cereb Blood Flow Metab* [Internet]. 2015;35:412–23.
52
53 1009 Available from: <http://www.ncbi.nlm.nih.gov/pubmed/25515214>
54
55
56 1010 41. Dong H, Wang C, Lu S, Yu C, Huang L, Feng W, et al. A panel of four decreased serum
57
58 1011 microRNAs as a novel biomarker for early Parkinson’s disease. *Biomarkers* [Internet].
59
60
61
62
63
64
65

1
2
3
4 1012 2016;21:129–37. Available from: <http://www.ncbi.nlm.nih.gov/pubmed/26631297>
5
6
7 1013 42. Fang Y, Fullwood MJ. Roles, Functions, and Mechanisms of Long Non-coding RNAs in
8
9 1014 Cancer. *Genomics Proteomics Bioinforma* [Internet]. 2016;14:42–54. Available from:
10
11
12 1015 <http://www.ncbi.nlm.nih.gov/pubmed/26883671>
13
14 1016 43. Li H, Yao G, Zhai J, Hu D, Fan Y. LncRNA FTX Promotes Proliferation and Invasion of
15
16 1017 Gastric Cancer via miR-144/ZFX Axis. *Onco Targets Ther* [Internet]. 2019;12:11701–13.
17
18
19 1018 Available from: <http://www.ncbi.nlm.nih.gov/pubmed/32021248>
20
21 1019 44. Widlansky ME, Jensen DM, Wang J, Liu Y, Geurts AM, Kriegel AJ, et al. miR-29
22
23
24 1020 contributes to normal endothelial function and can restore it in cardiometabolic disorders. *EMBO*
25
26 1021 *Mol Med* [Internet]. 2018;10. Available from: <http://www.ncbi.nlm.nih.gov/pubmed/29374012>
27
28
29 1022 45. Li X, Zhao Q, Qi J, Wang W, Zhang D, Li Z, et al. lncRNA Ftx promotes aerobic glycolysis
30
31 1023 and tumor progression through the PPARgamma pathway in hepatocellular carcinoma. *Int J*
32
33
34 1024 *Oncol* [Internet]. 2018;53:551–66. Available from:
35
36 1025 <http://www.ncbi.nlm.nih.gov/pubmed/29845188>
37
38 1026 46. Klotz L, Diehl L, Dani I, Neumann H, von Oppen N, Dolf A, et al. Brain endothelial
39
40
41 1027 PPARgamma controls inflammation-induced CD4+ T cell adhesion and transmigration in vitro. *J*
42
43 1028 *Neuroimmunol* [Internet]. 2007;190:34–43. Available from:
44
45
46 1029 <http://www.ncbi.nlm.nih.gov/pubmed/17719655>
47
48 1030 47. Ramirez SH, Heilman D, Morse B, Potula R, Haorah J, Persidsky Y. Activation of
49
50
51 1031 peroxisome proliferator-activated receptor gamma (PPARgamma) suppresses Rho GTPases in
52
53 1032 human brain microvascular endothelial cells and inhibits adhesion and transendothelial migration
54
55 1033 of HIV-1 infected monocytes. *J Immunol* [Internet]. 2008;180:1854–65. Available from:
56
57
58 1034 <http://www.ncbi.nlm.nih.gov/pubmed/18209083>
59
60
61
62
63
64
65

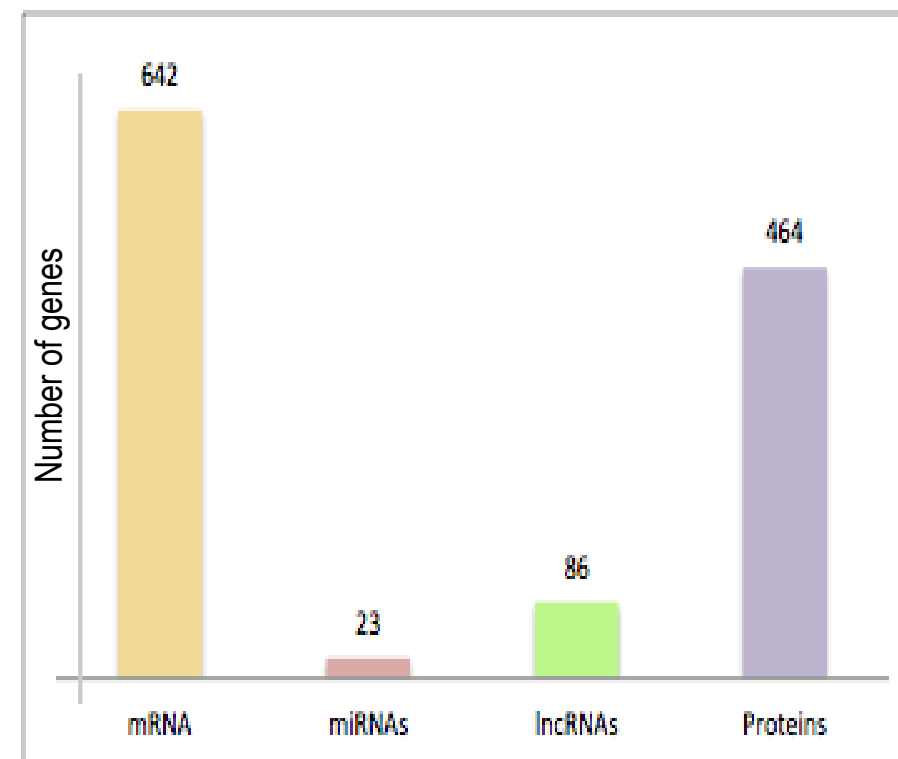
1
2
3
4 1035 48. Choy KW, Murugan D, Leong XF, Abas R, Alias A, Mustafa MR. Flavonoids as Natural
5
6
7 1036 Anti-Inflammatory Agents Targeting Nuclear Factor-Kappa B (NFkappaB) Signaling in
8
9 1037 Cardiovascular Diseases: A Mini Review. *Front Pharmacol* [Internet]. 2019;10:1295. Available
10
11
12 1038 from: <http://www.ncbi.nlm.nih.gov/pubmed/31749703>
13
14 1039 49. Figueira I, Garcia G, Pimpao RC, Terrasso AP, Costa I, Almeida AF, et al. Polyphenols
15
16 1040 journey through blood-brain barrier towards neuronal protection. *Sci Rep* [Internet].
17
18
19 1041 2017;7:11456. Available from: <http://www.ncbi.nlm.nih.gov/pubmed/28904352>
20
21 1042 50. Wimmer I, Tietz S, Nishihara H, Deutsch U, Sallusto F, Gosselet F, et al. PECAM-1
22
23
24 1043 Stabilizes Blood-Brain Barrier Integrity and Favors Paracellular T-Cell Diapedesis Across the
25
26 1044 Blood-Brain Barrier During Neuroinflammation. *Front Immunol* [Internet]. 2019;10:711.
27
28
29 1045 Available from: <http://www.ncbi.nlm.nih.gov/pubmed/31024547>
30
31 1046 51. Chistiakov DA, Orekhov AN, Bobryshev Y V. Effects of shear stress on endothelial cells: go
32
33
34 1047 with the flow. *Acta Physiol* [Internet]. 2017;219:382–408. Available from:
35
36 1048 <http://www.ncbi.nlm.nih.gov/pubmed/27246807>
37
38 1049 52. Izawa Y, Gu YH, Osada T, Kanazawa M, Hawkins BT, Koziol JA, et al. beta1-integrin-
39
40
41 1050 matrix interactions modulate cerebral microvessel endothelial cell tight junction expression and
42
43 1051 permeability. *J Cereb Blood Flow Metab* [Internet]. 2018;38:641–58. Available from:
44
45
46 1052 <http://www.ncbi.nlm.nih.gov/pubmed/28787238>
47
48 1053 53. Zhang Y, Huang W. Transforming Growth Factor beta1 (TGF-beta1)-Stimulated Integrin-
49
50
51 1054 Linked Kinase (ILK) Regulates Migration and Epithelial-Mesenchymal Transition (EMT) of
52
53 1055 Human Lens Epithelial Cells via Nuclear Factor kappaB (NF-kappaB). *Med Sci Monit* [Internet].
54
55 1056 2018;24:7424–30. Available from: <http://www.ncbi.nlm.nih.gov/pubmed/30332398>
56
57
58 1057
59
60
61
62
63
64
65

Figure 1. TNFa modulates the expression of mRNAs, miRNAs, IncRNAs and proteins in human brain microvascular endothelial cells.

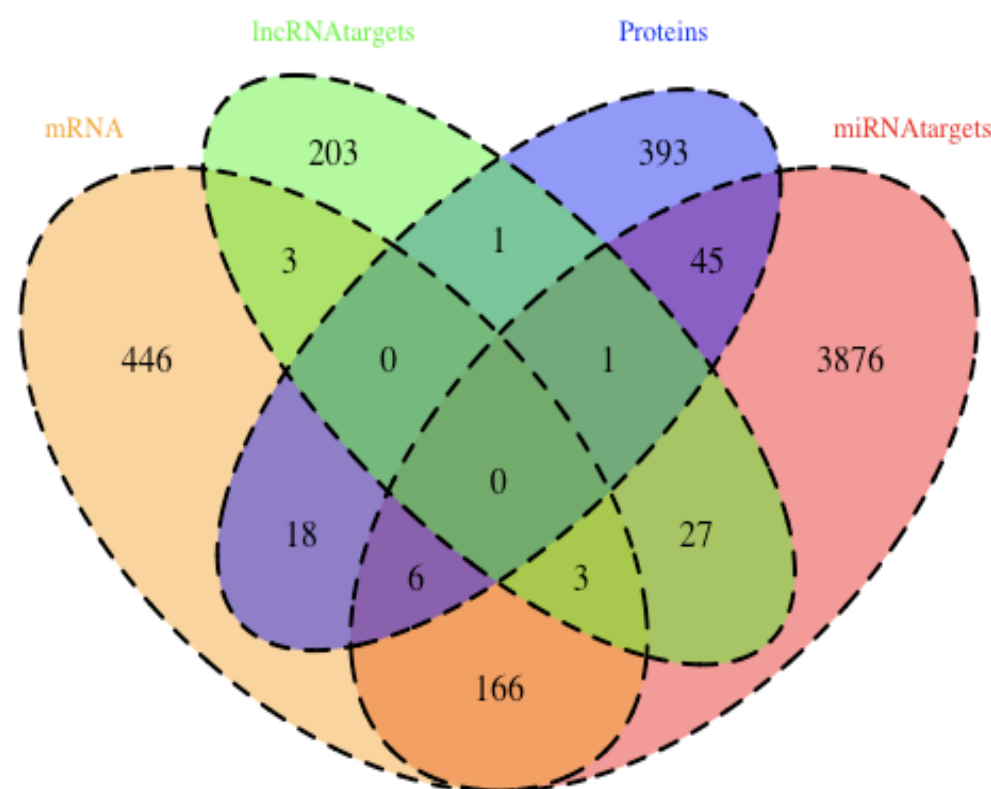
A)



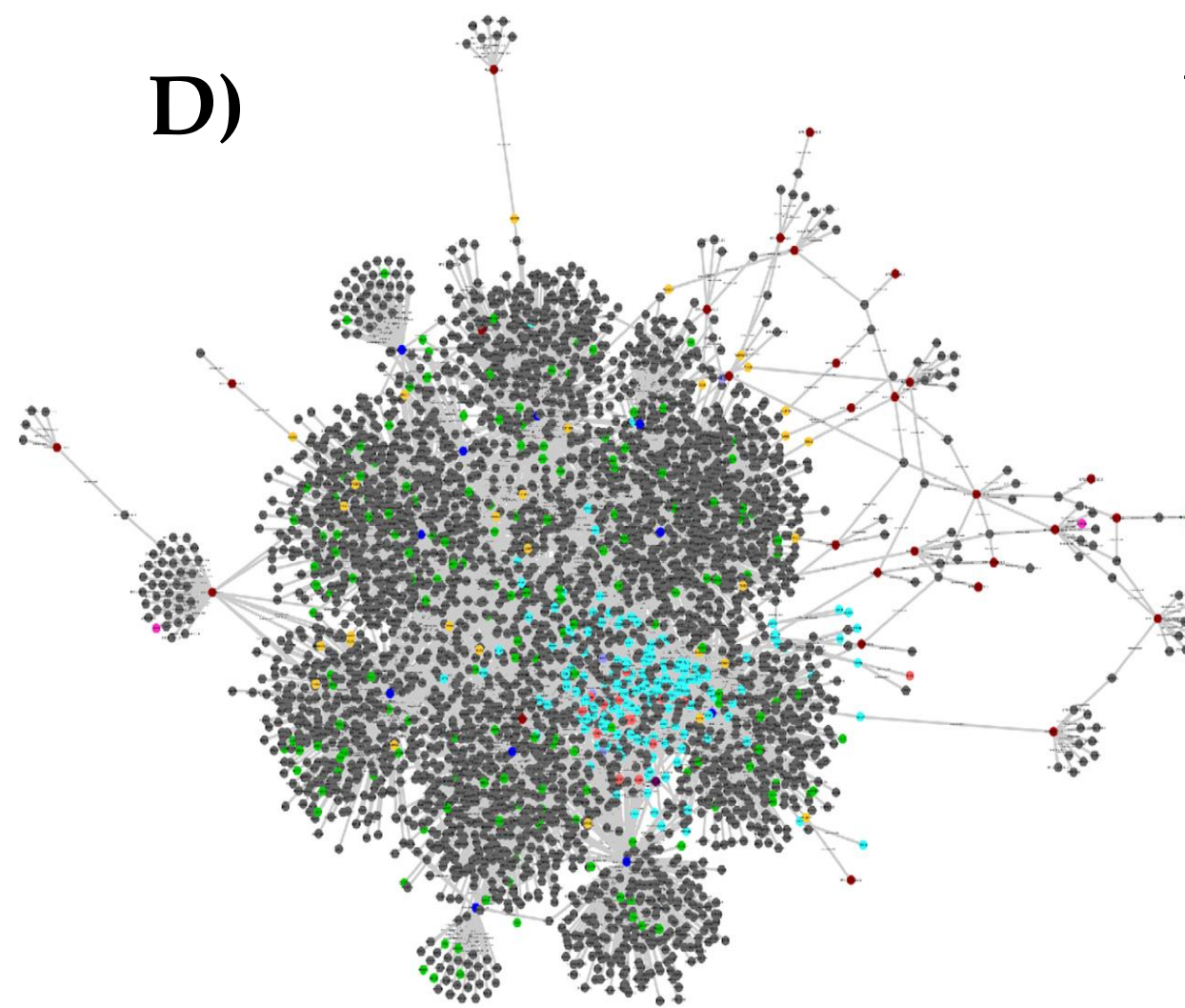
B)



C)



D)



E)

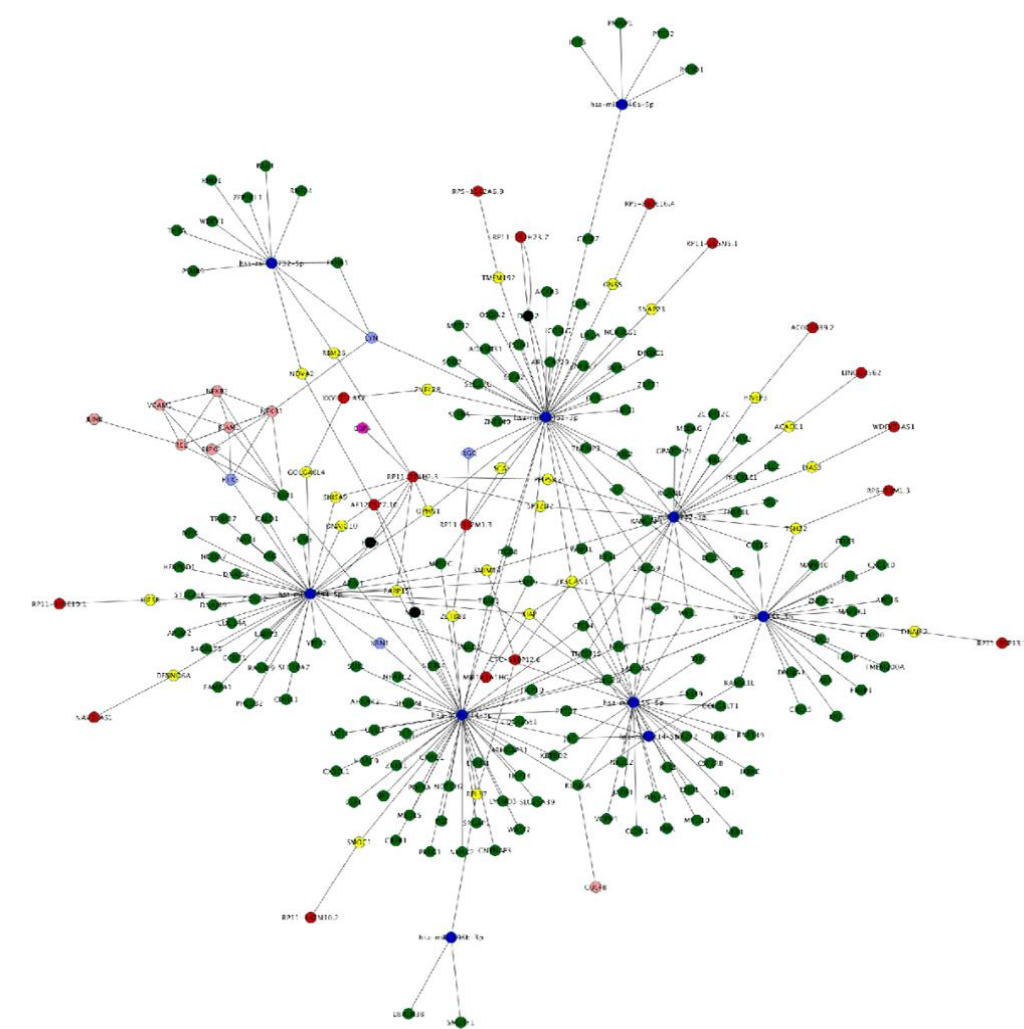
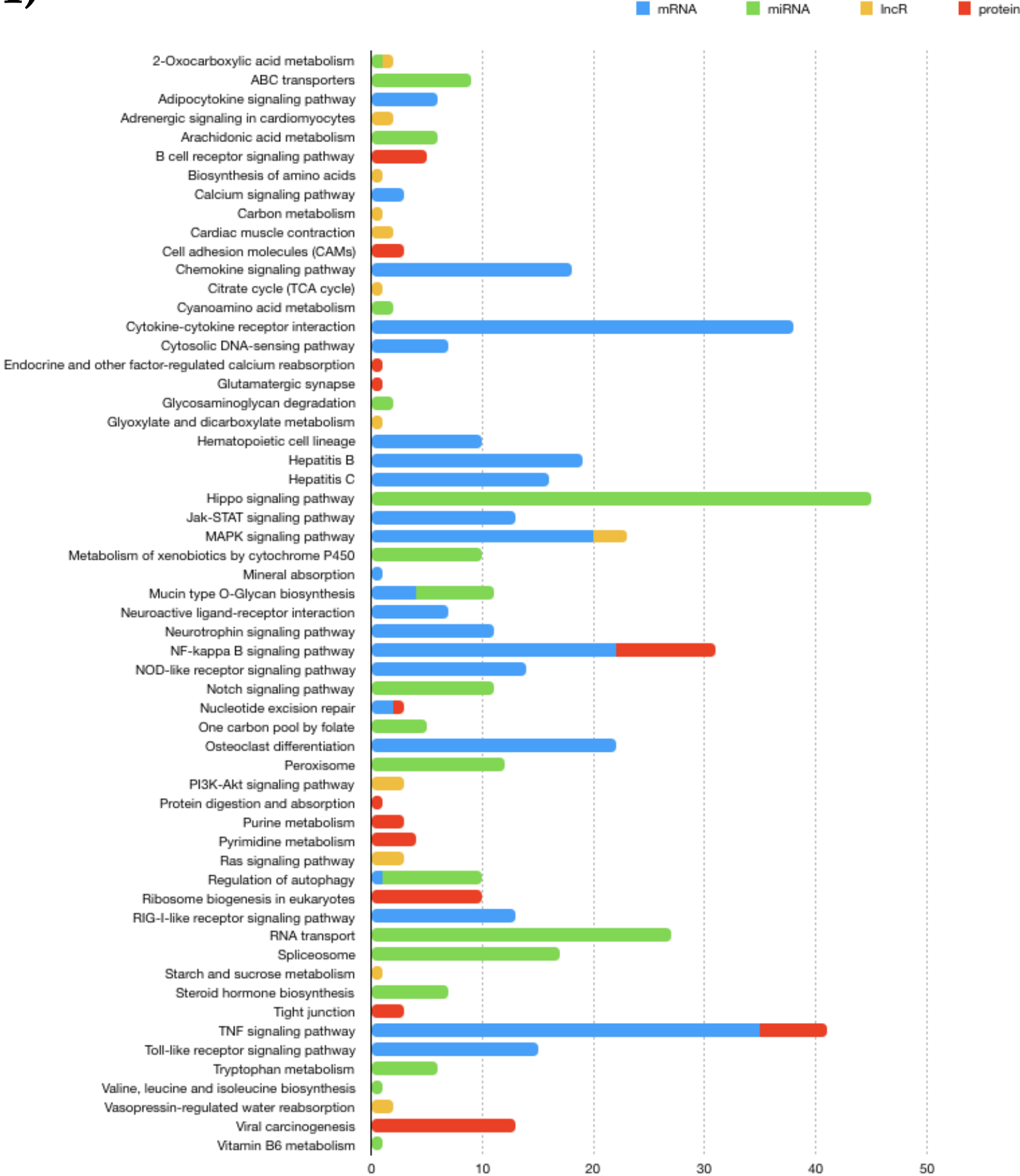


Figure 2. Enriched pathways of differentially expressed transcripts and proteins of HBMEC cells treated with TNFa vs control.

A)



B)

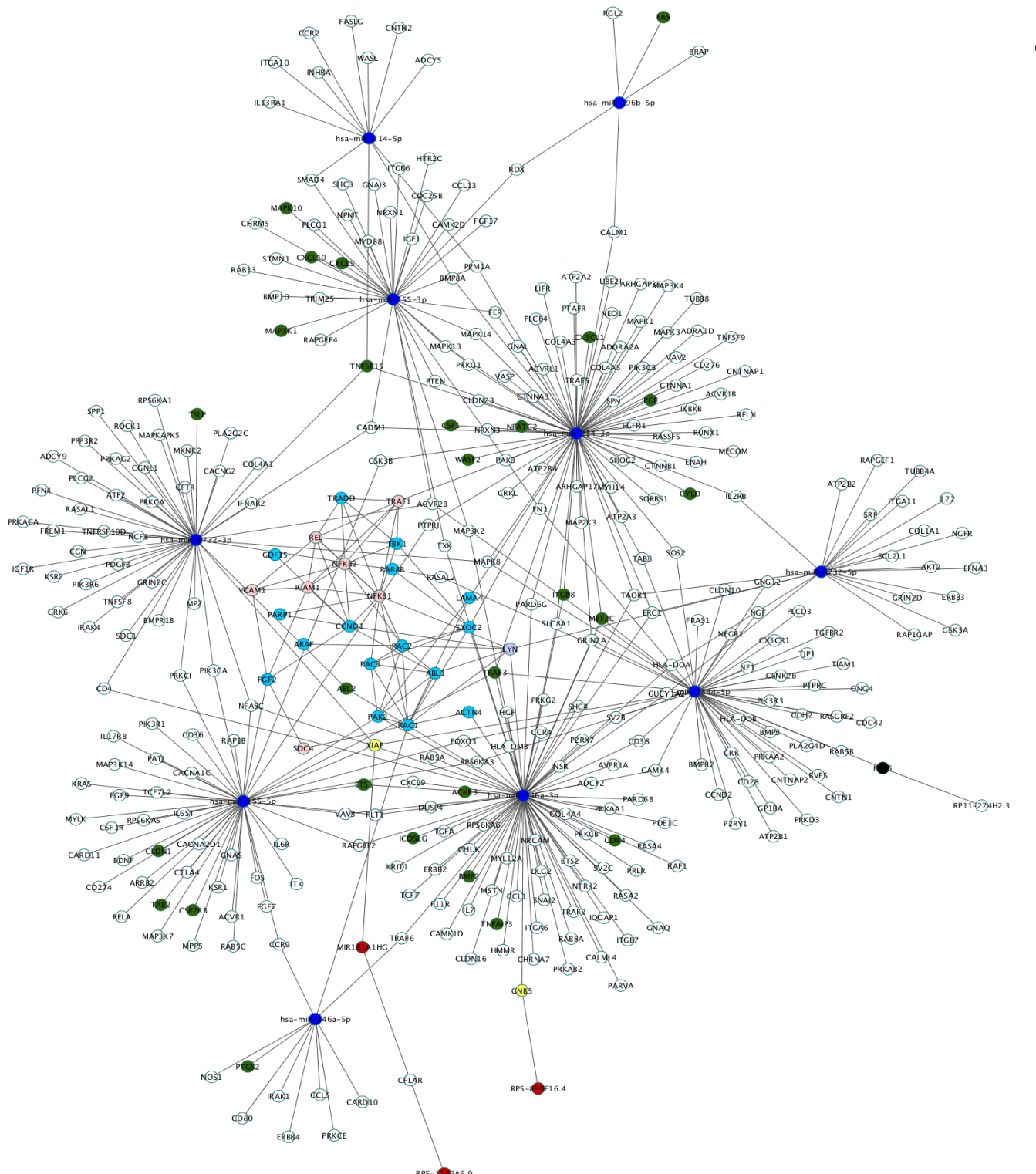


Figure 3. Genomic modifications induced by valerolactones treatment in HBMEC cells.

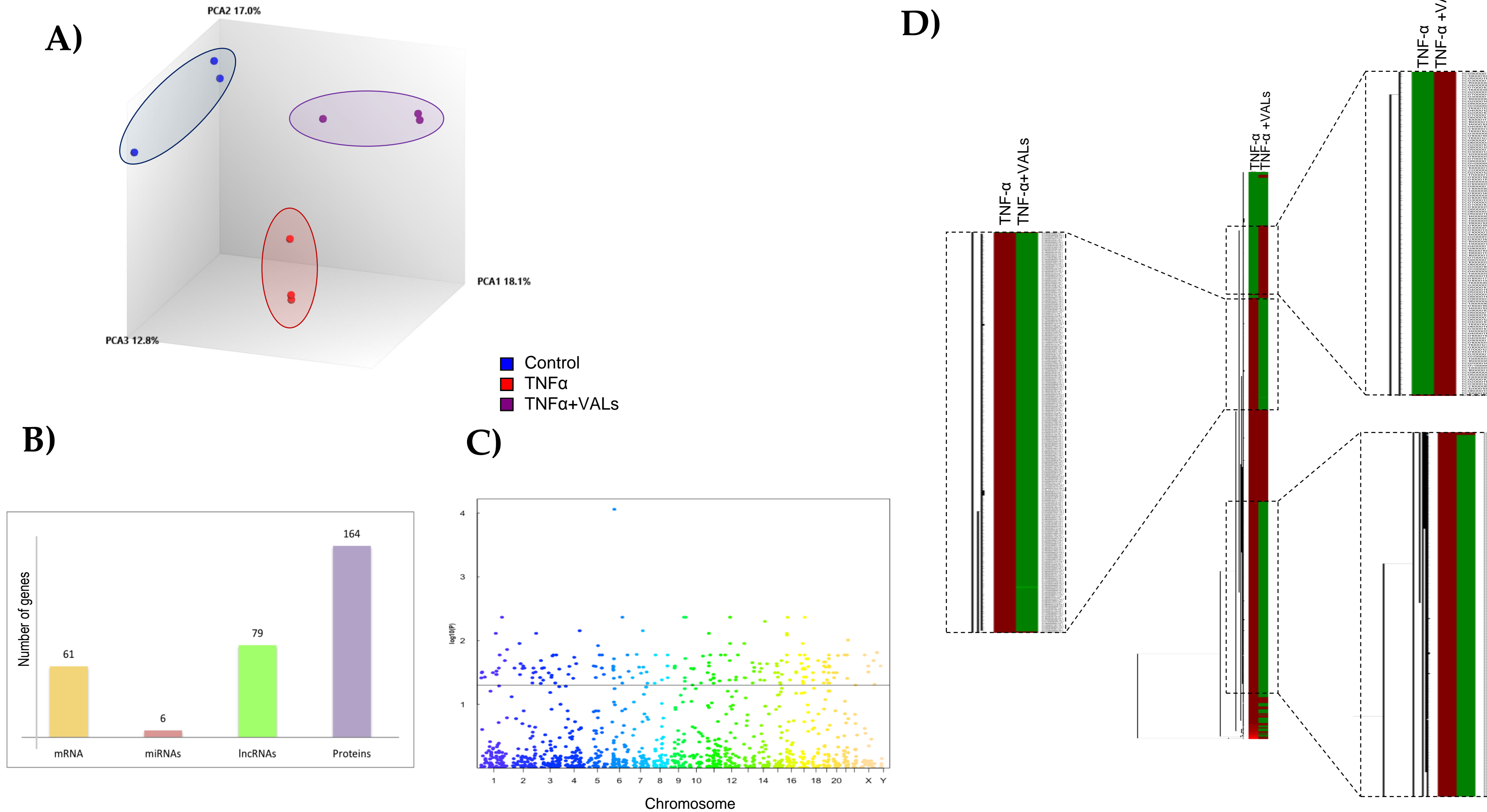
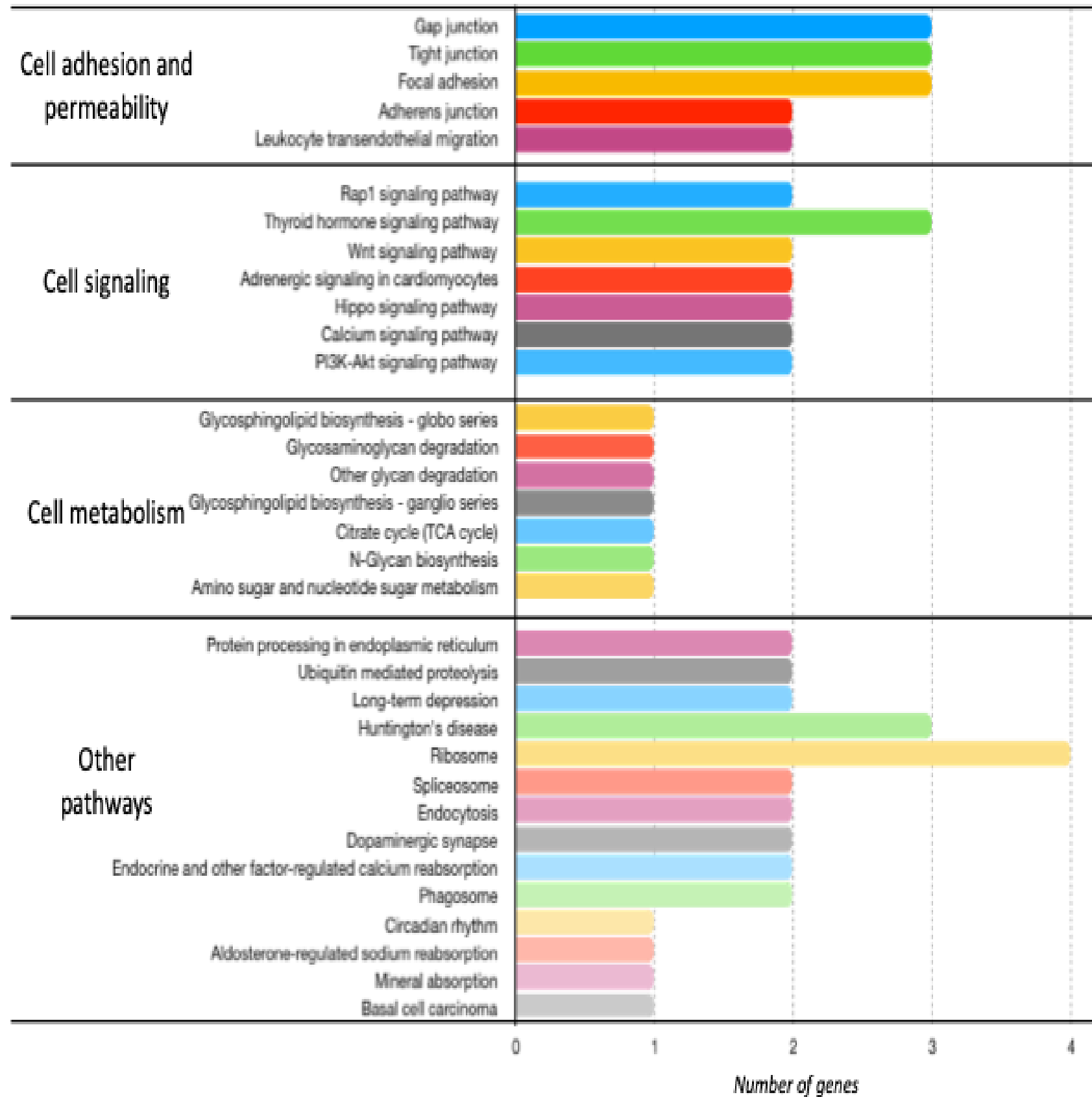


Figure 4. Enriched pathways of protein-coding genes differentially expressed in HBMEC cells treated with valerolactones.

A)



B)

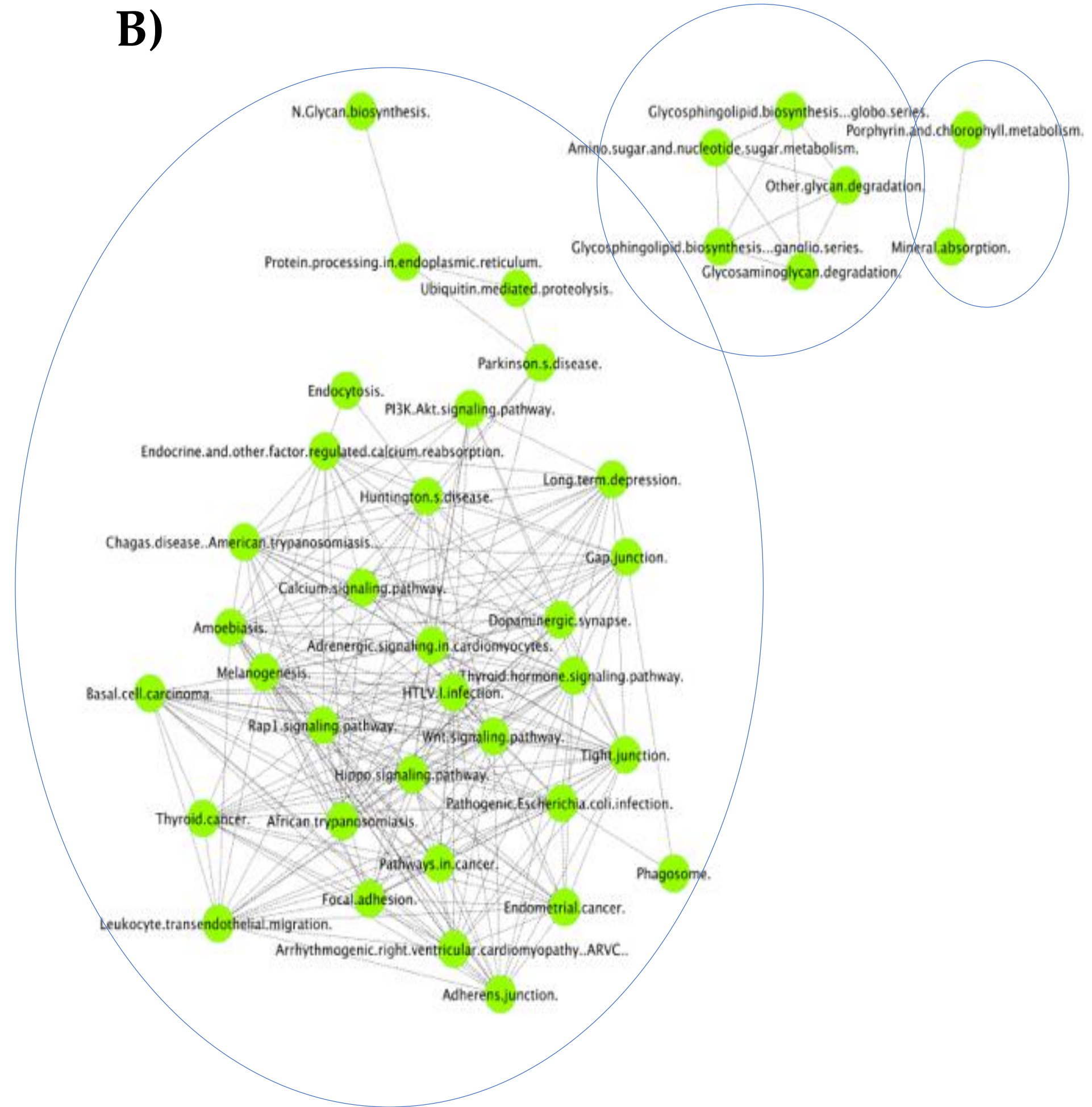
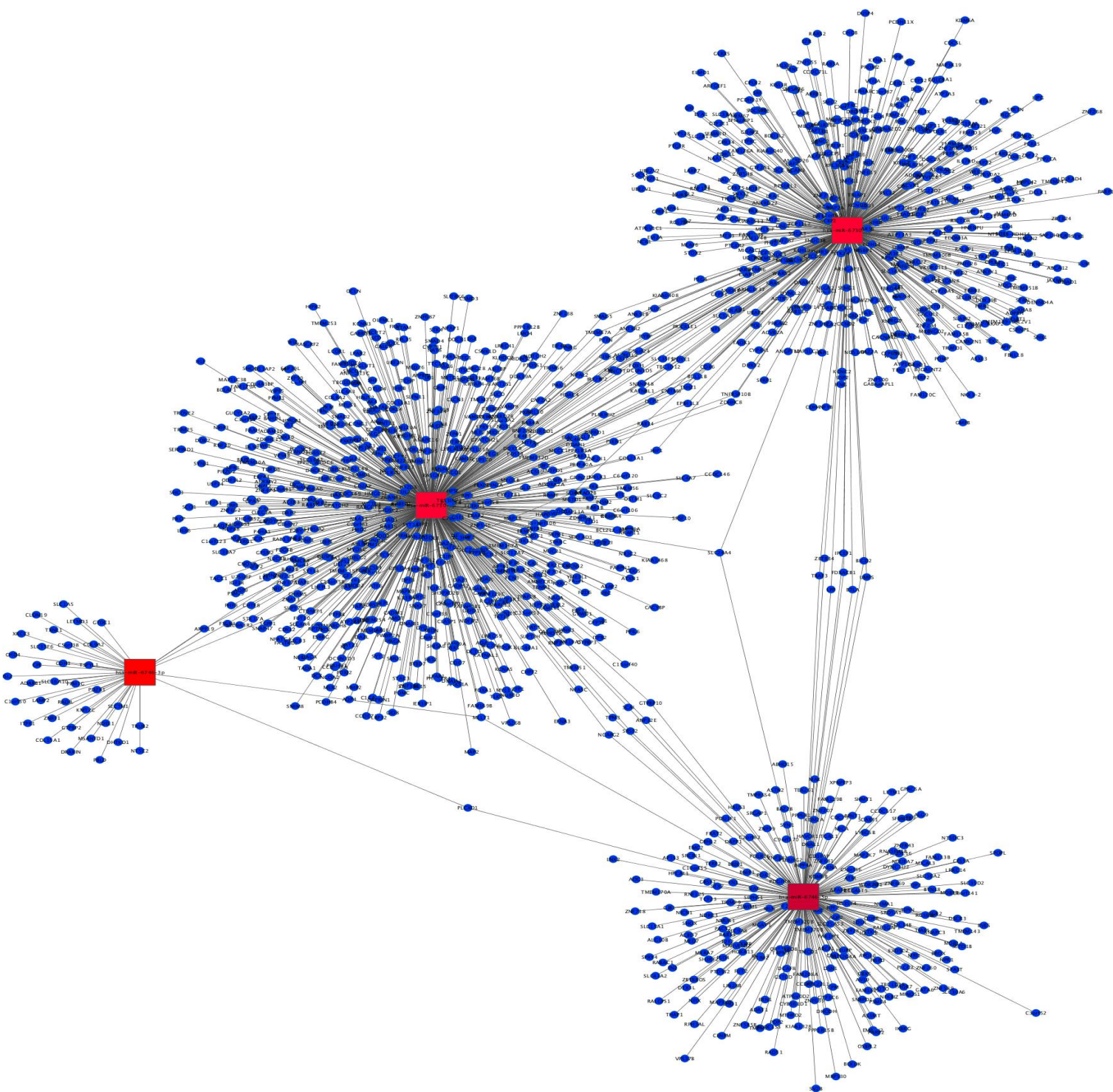


Figure 5. miRNAs expression mediated by valerolactones treatment in HBMEC cell and their relation with endothelial functions.

A)



B)

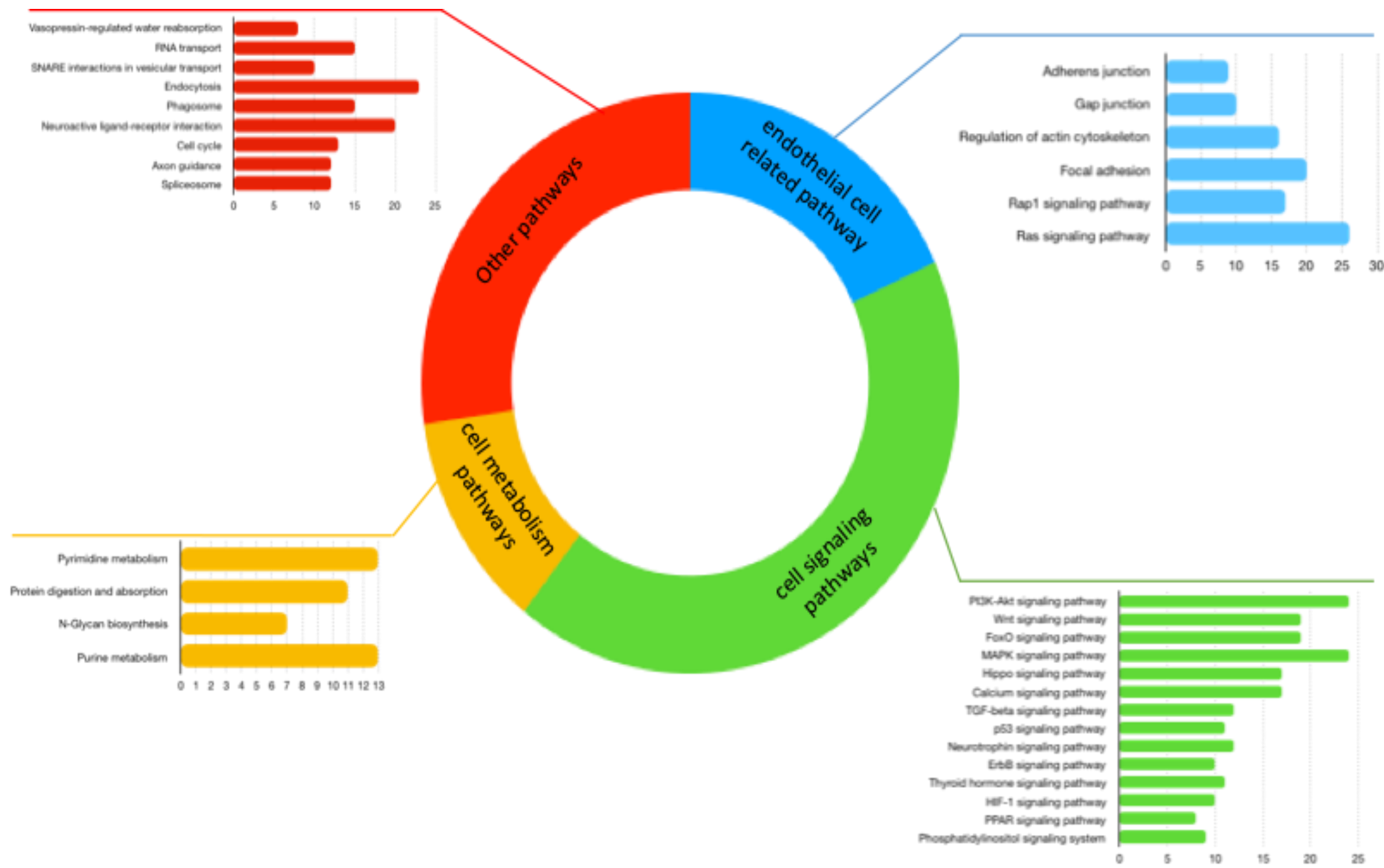
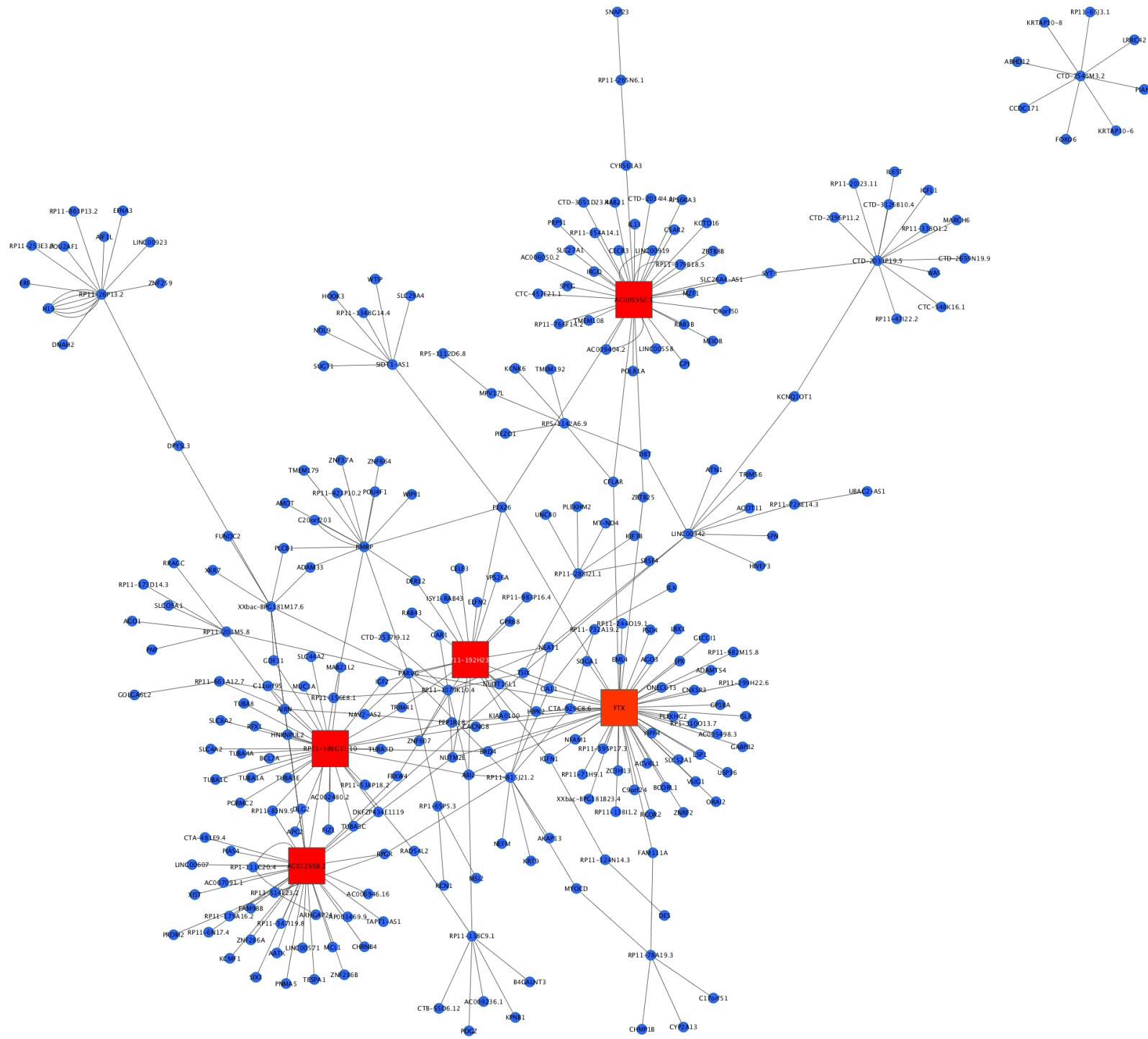
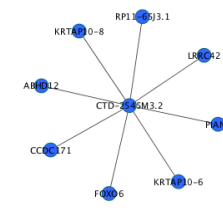


Figure 6. IncRNAs expression mediated by valerolactones treatment in HBMEC cell and their relation with endothelial cell functions.

A)



B)



C)

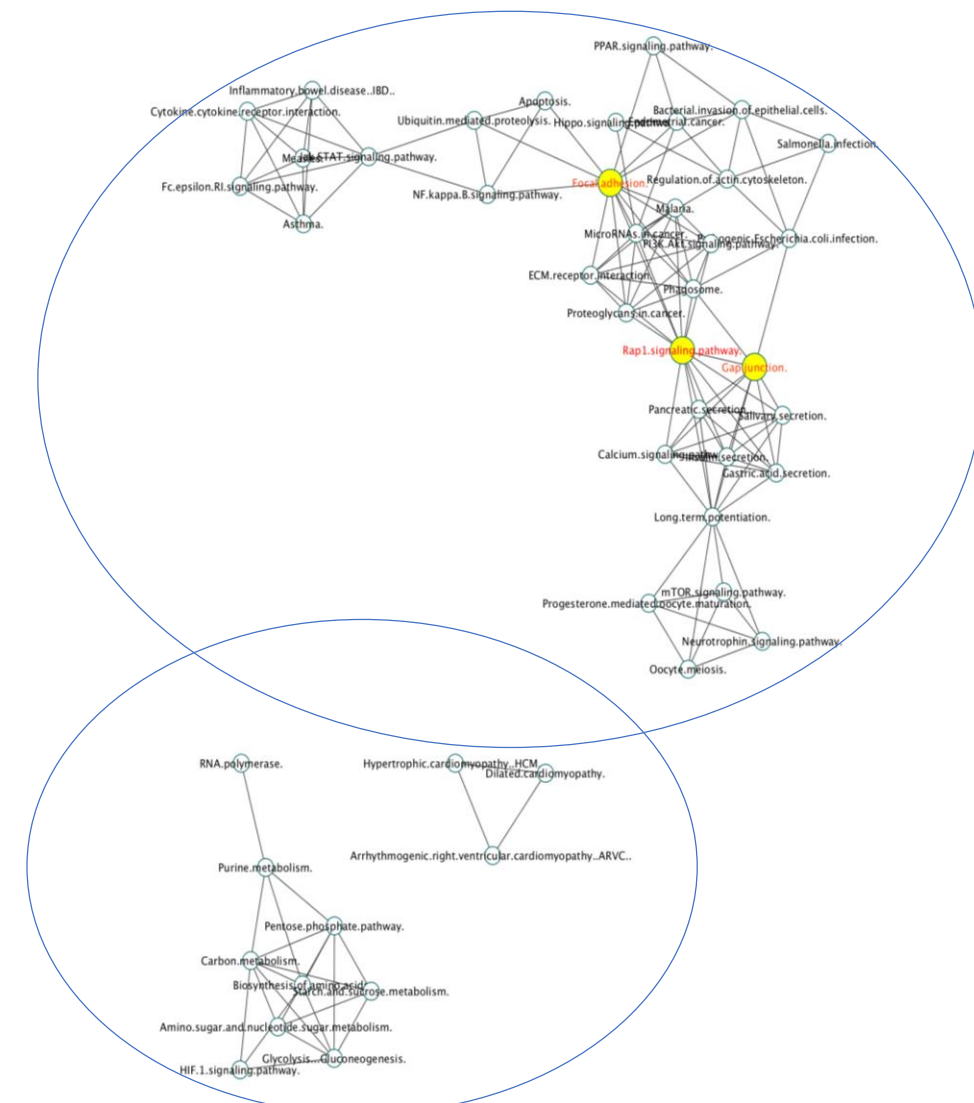
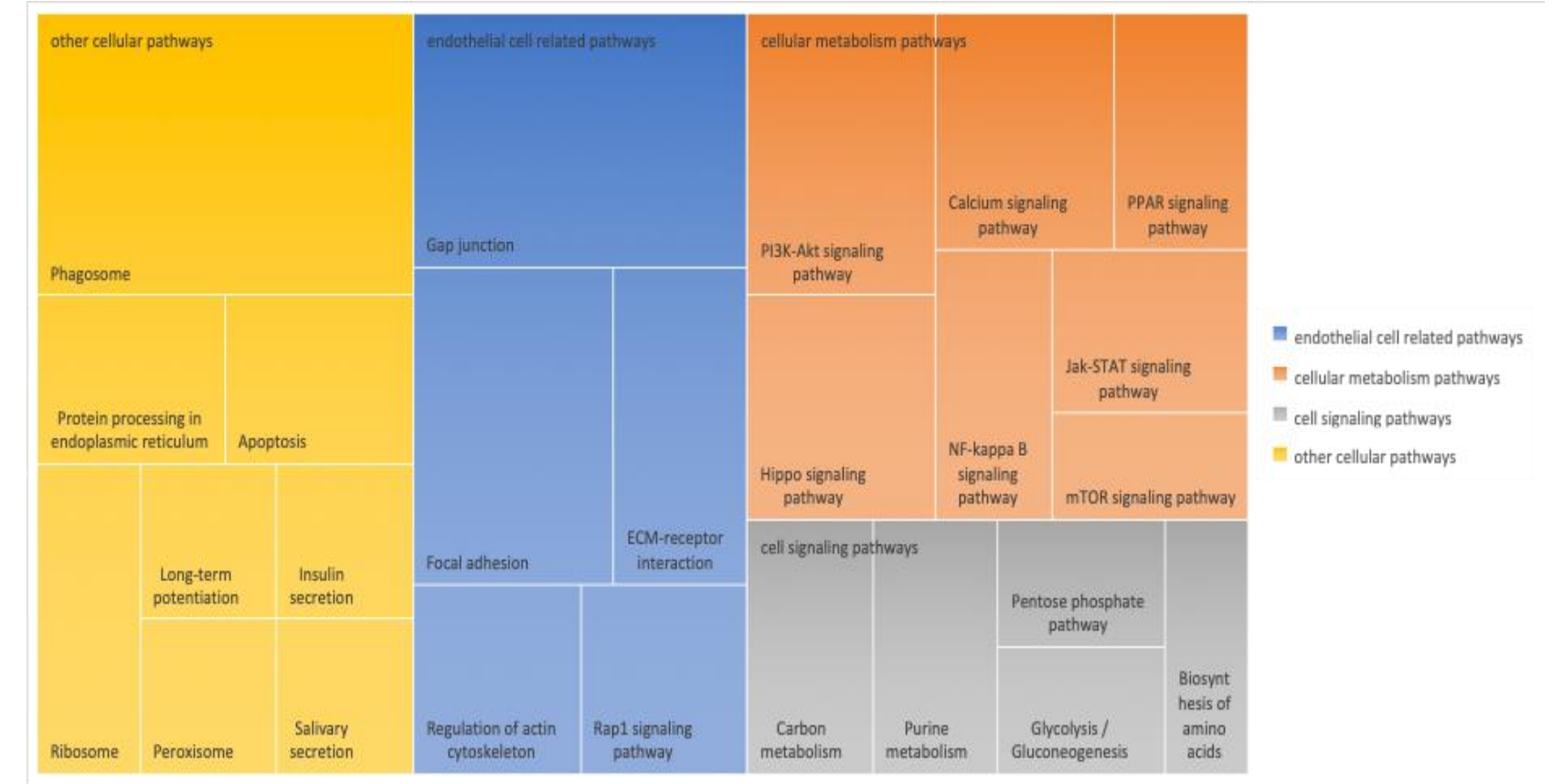
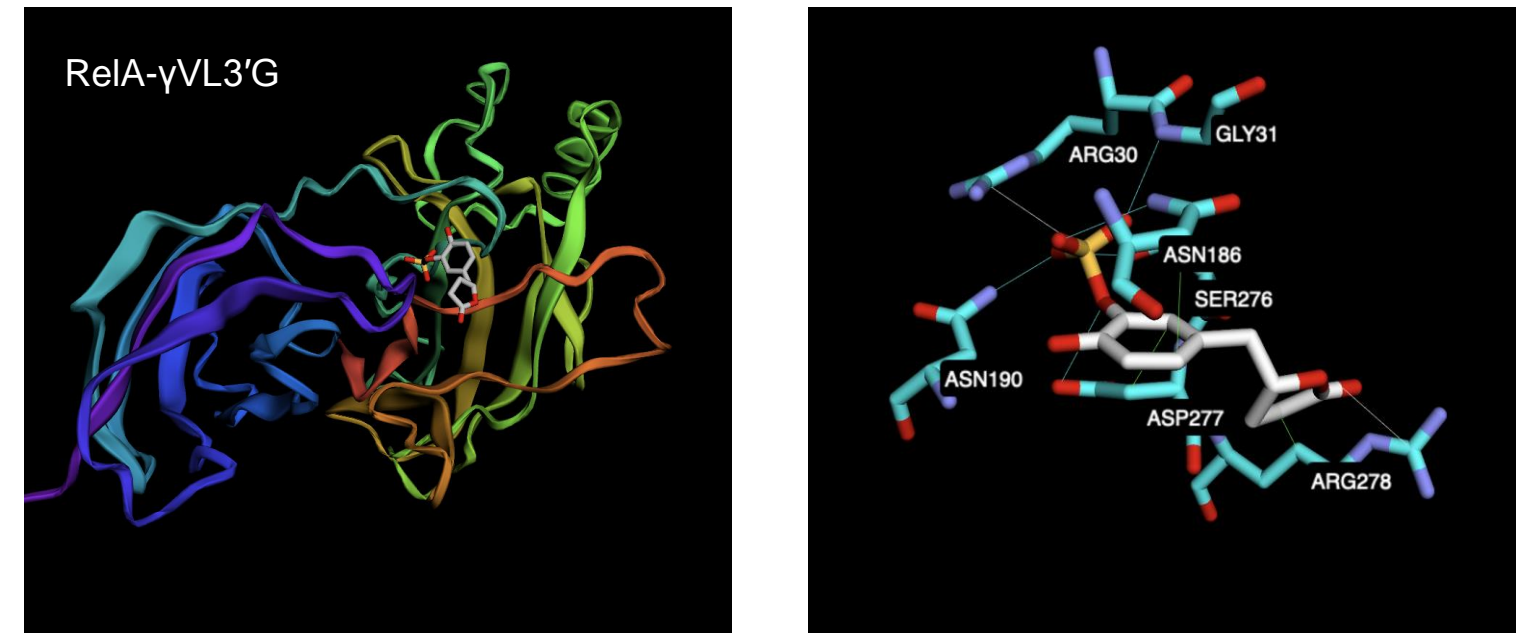


Figure 8. Docking

A)

Transcription factor	P-value	Adjusted p-value
NFKB	7.64E-21	2.18E-18
RELA	5.39E-21	3.08E-18
JUN	2.41E-07	0.00001966
STAT2	0.000004974	0.0003156
IRF1	0.000004636	0.0003309
STAT1	0.00001196	0.0006207
FOXO4	0.00007812	0.003717
ATF2	0.0001153	0.005064
SRF	0.0001429	0.00583
STAT3	0.0001939	0.00738
EGR1	0.0003295	0.01176
ZNF382	0.0009342	0.02963
JUND	0.00109	0.03276
ATF4	0.001306	0.03551
HIVEP2	0.002073	0.04933

B)



C)

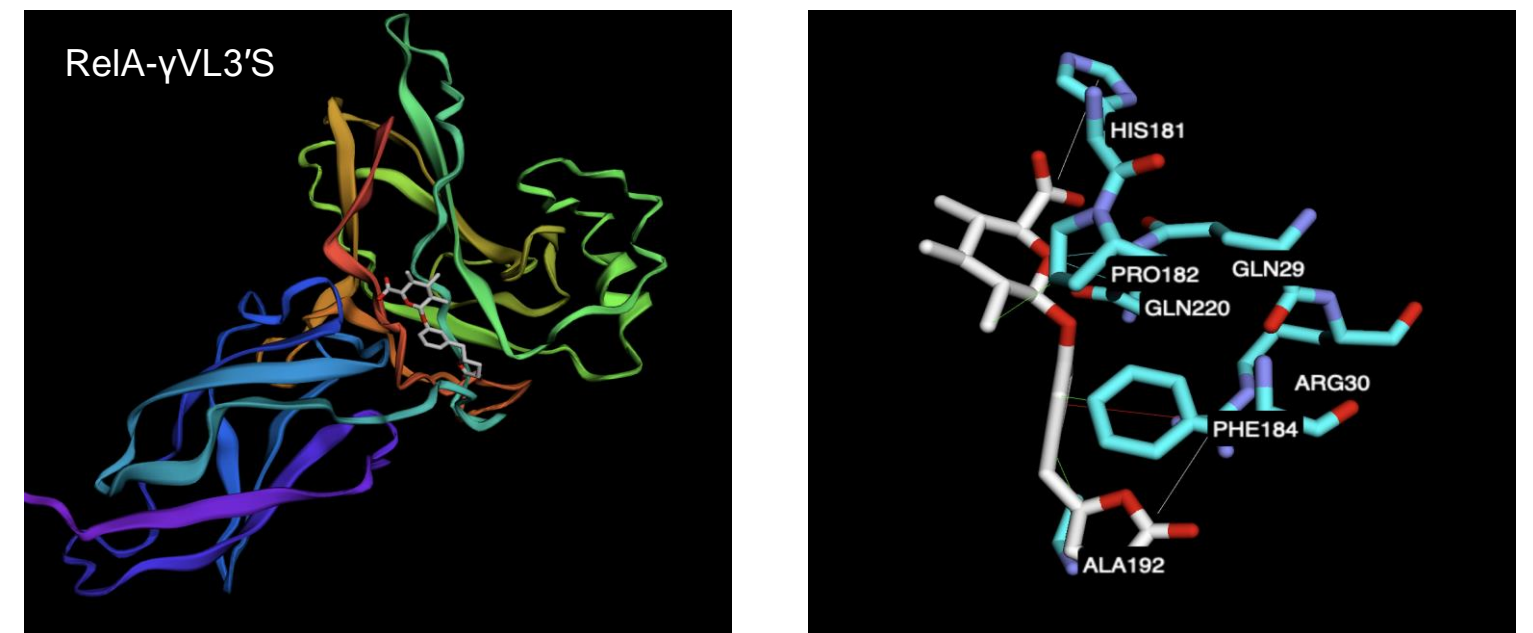
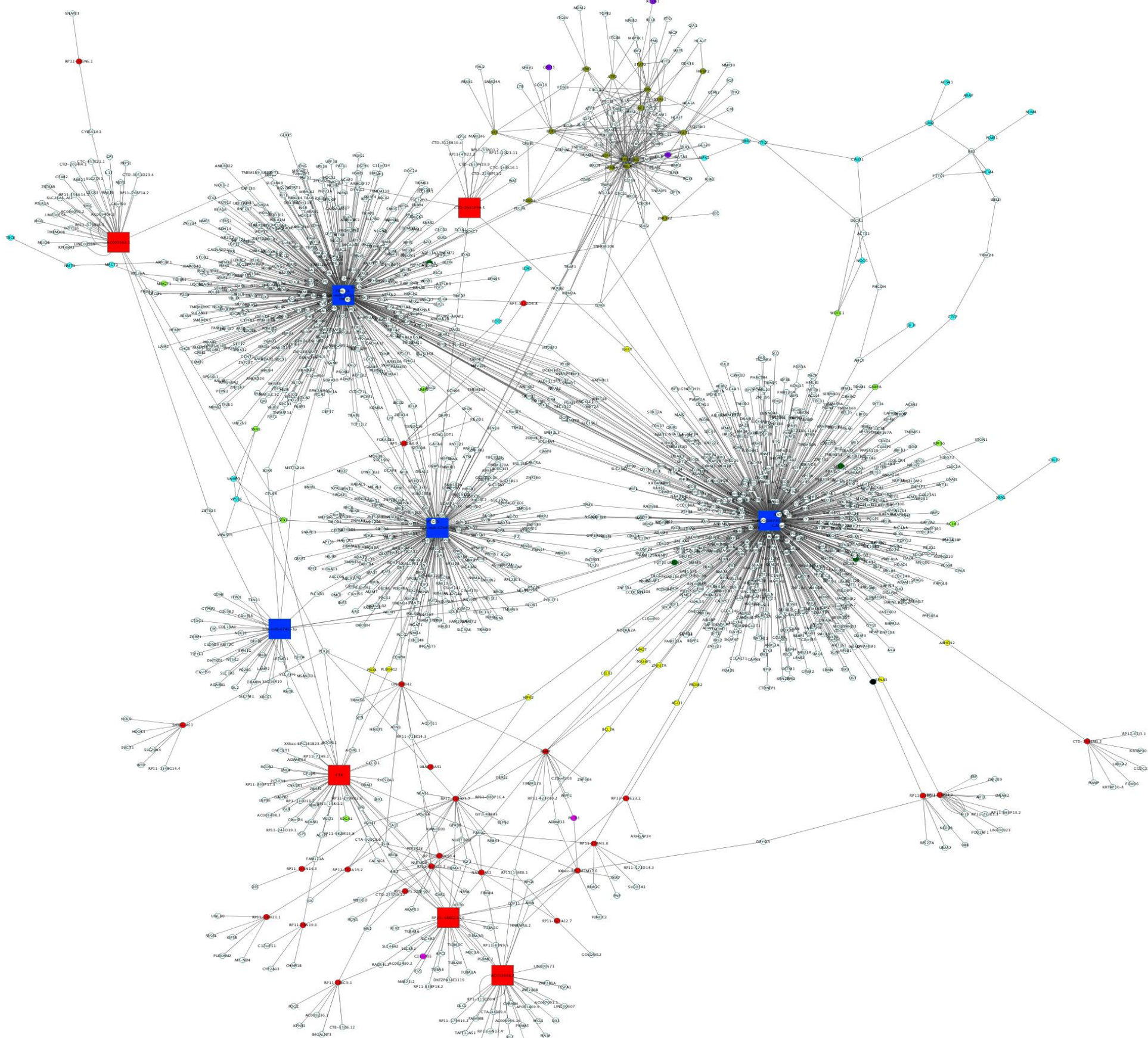
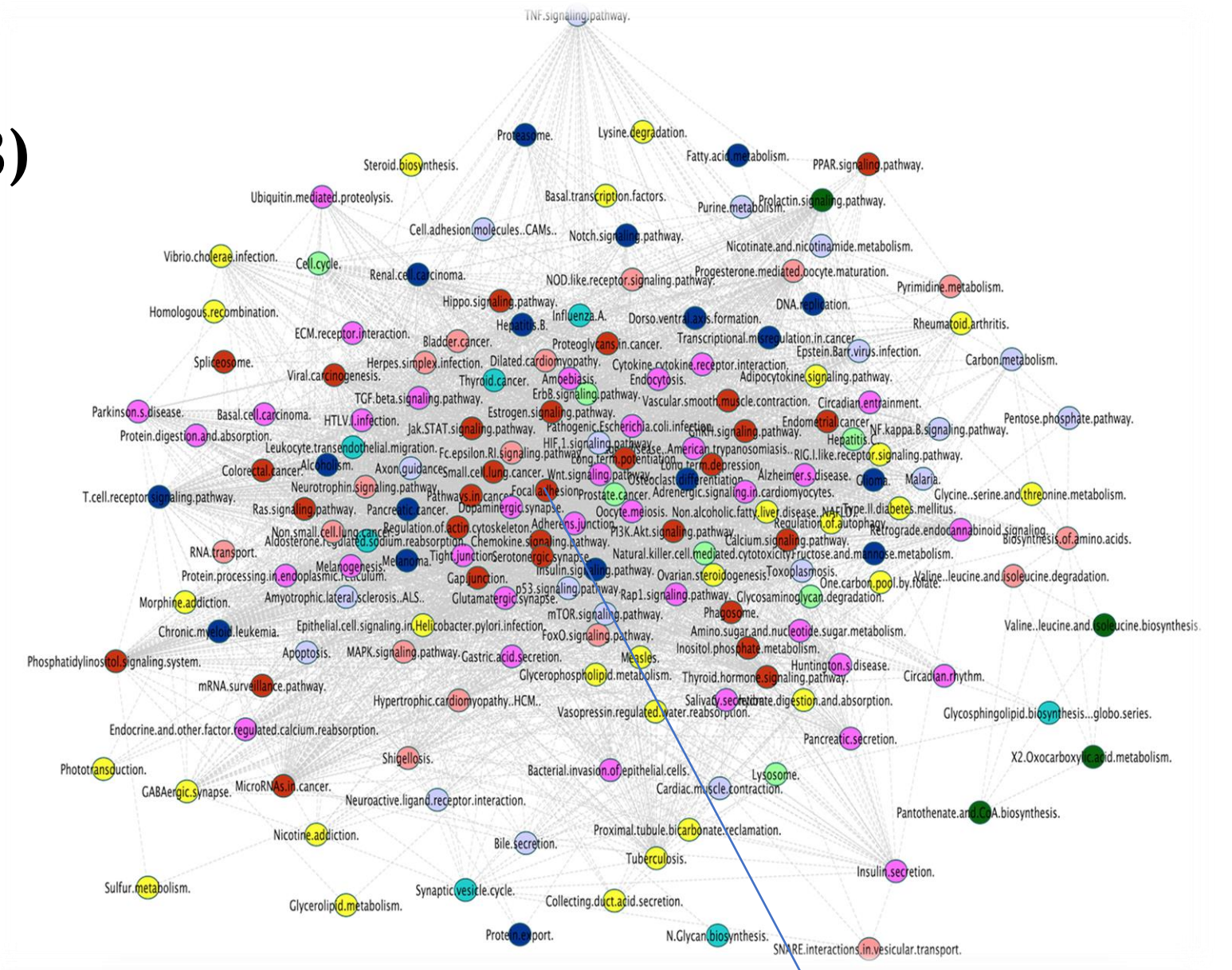


Figure 9. Global network of interactions modulated by valerolactones treatment in HBMEC cells and their relation with endothelial function.

A)



B)



C)

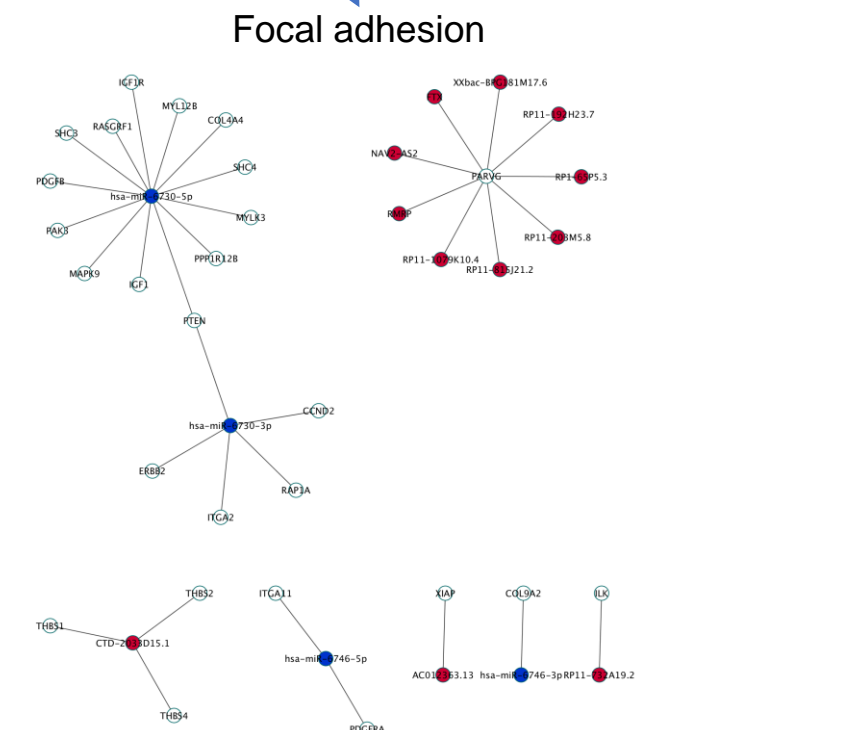
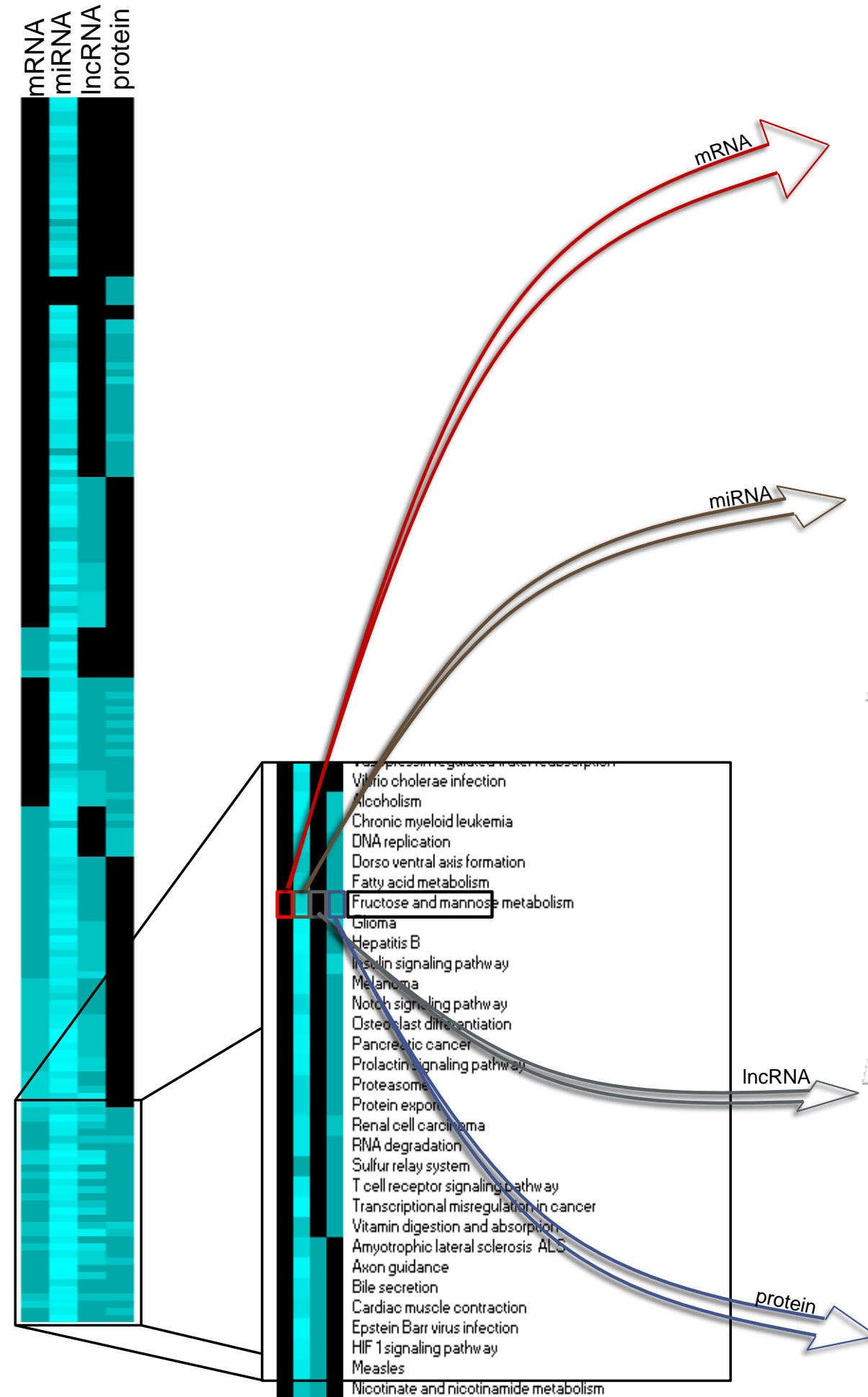


Figure 10. Integration of differentially expressed mRNAs, microRNA target gene, lncRNA target gene and protein modulating focal adhesion function in HBMEC cells treated with valerolactones.

A)



B)

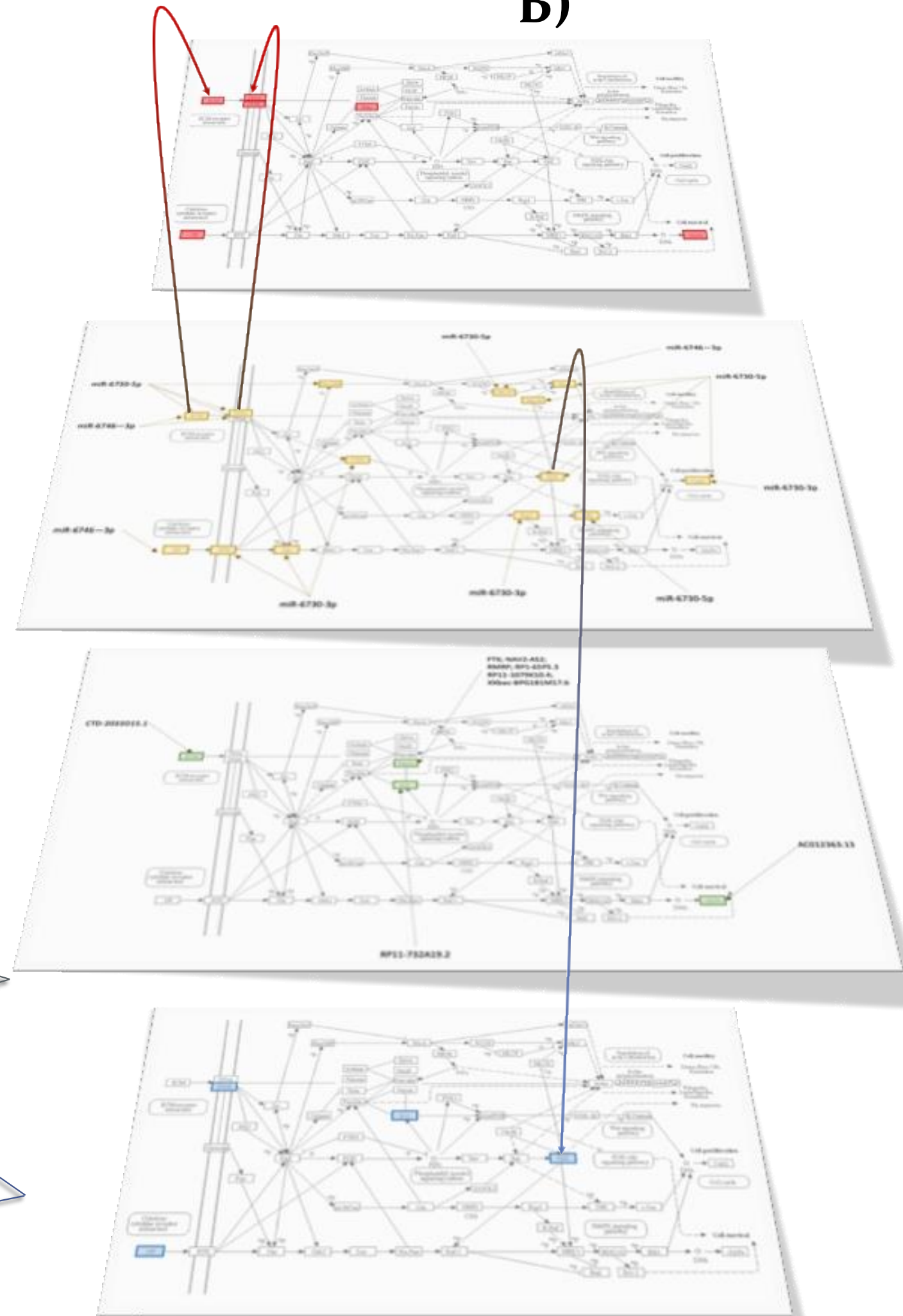
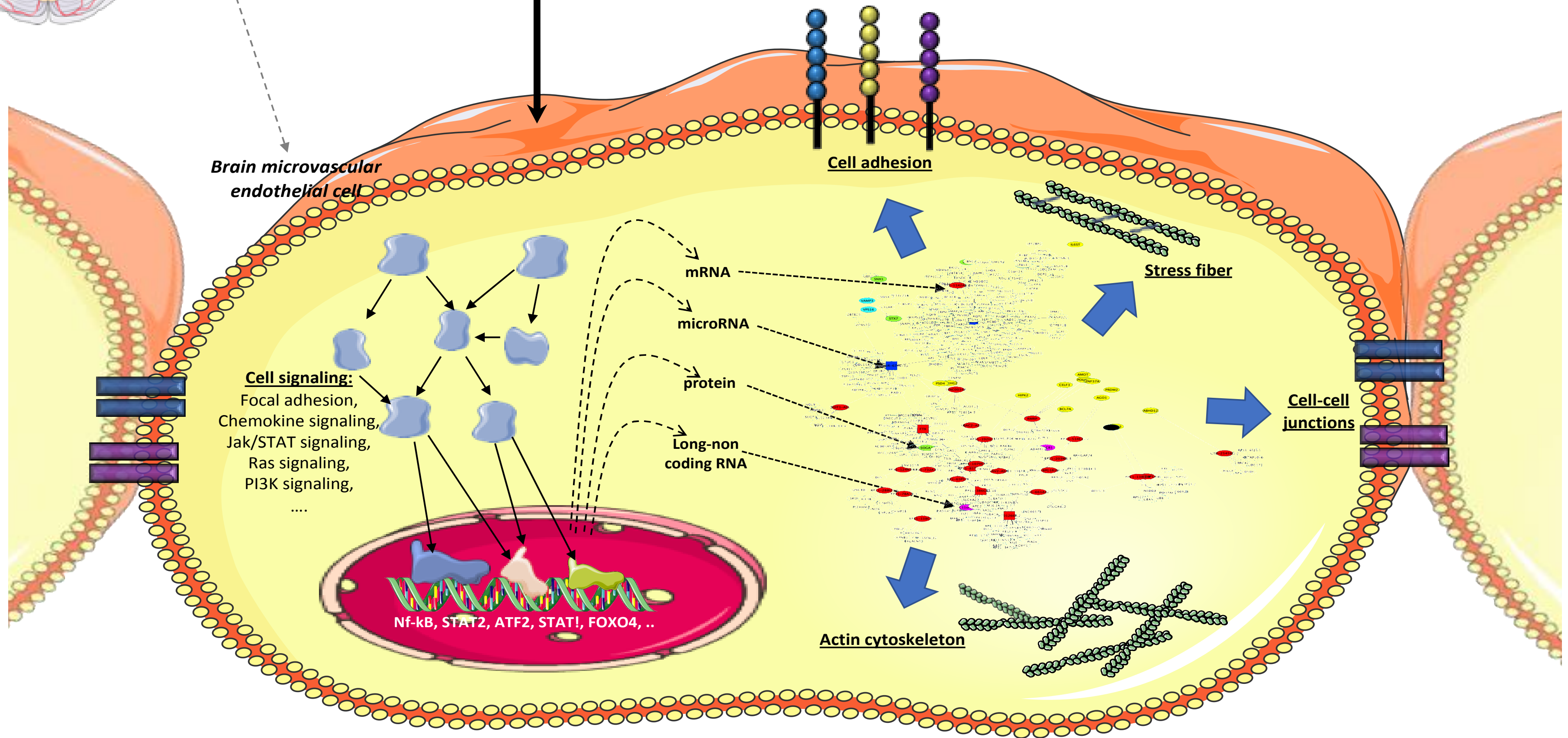
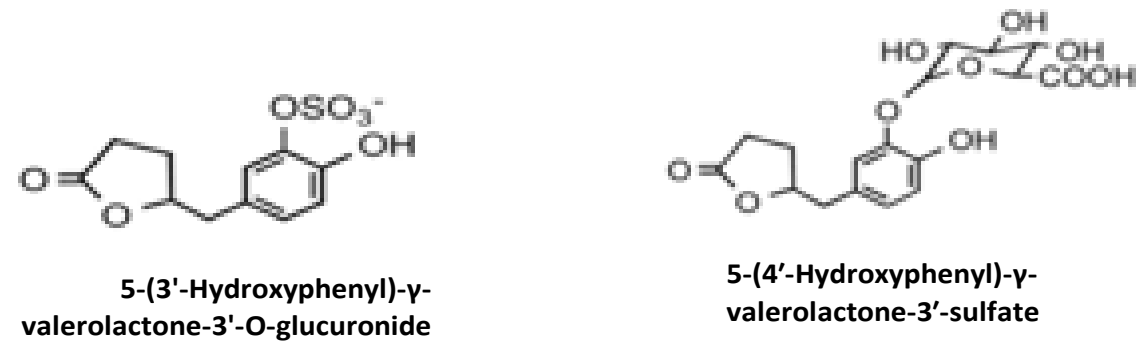
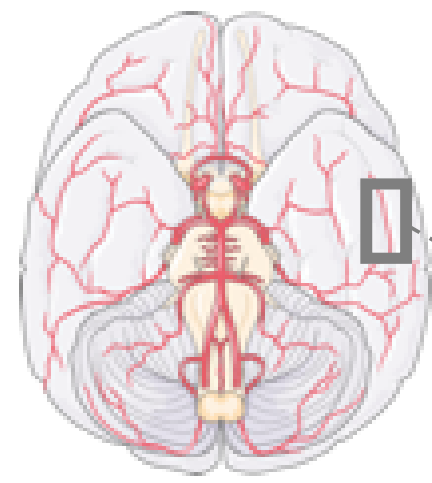



Figure 11







Click here to access/download
Supplementary Material
Supplemental_Table_2.xlsx





Click here to access/download
Supplementary Material
Supplemental_Table_3.xlsx







Click here to access/download
Supplementary Material
supp figures.pptx

